Supplementary Information

Coumarin functionalized NIR fluorescent probe based on thiopyrone skeleton for the detection of Cys and its applications

Huan Zhang, Baoze Guo, Junqing Zhou, Cong Sun, Jinwei Zhang, Shuai Guo, Songhua Zhu, Youlai Zhang*

Tianjin Key Laboratory of Organic Solar Cells and Photochemical Conversion, School of Chemistry and Chemical Engineering, Tianjin University of Technology, Tianjin 300384, P. R. China.

Figure S14. TOF-MS spectra of compound **2**.

Figure S15. TOF-MS spectra of compound **3**.

Figure S16. TOF-MS spectra of compound **4**.

Figure S17. TOF-MS spectra of compound PH-OH.

Figure S18. TOF-MS spectra of compound PH-Cys.

Figure S19. (a) UV-vis absorption spectral responses of probe PH-Cys towards Cys. **(b)** Fluorescence emission spectral responses of probe PH-Cys towards Cys. **(c)** Normalized Stokes shift diagram of probe PH-Cys (Stokes shift = 217 nm). **(d)** Color variations of PH-Cys upon Cys addition, and fluorescence variations of PH-Cys upon Cys addition under excitation with a 365 nm UV lamp.

Figure S20. (a) UV-vis absorption spectra for the time-dependent response of probe PH-Cys towards Cys. **(b)** Fluorescence emission spectra for the time-dependent response of probe PH-Cys towards Cys.

Figure S21. (a) UV-vis absorption spectra of probe PH-Cys for the concentration-dependent response towards Cys. **(b)** Fluorescence emission spectra of probe PH-Cys for the concentration-dependent response towards Cys. **(c)** Linear relationship between probe PH-Cys and Cys concentration. **(d)** CIE 1931 chromaticity coordinates (x, y) of probe PH-Cys at varying Cys concentrations.

Figure S22. (a) Fluorescence intensity at 779 nm of probe PH-Cys (10.0 μM) in the presence of various analytes in DMSO/PBS (7:3, v/v) at ambient temperature (all analytes were used at a concentration of 12.0 μM). **(b)** Fluorescence responses of probe PH-Cys (10.0 μM) towards various analytes. Black bars correspond to the addition of different analytes (12.0 μM) to the PH-Cys (10.0 μM) solution; red bars correspond to

the subsequent addition of cysteine (Cys) and other analytes (12.0 μM) to the aforementioned solution. **(c)** Color of the PH-Cys solution in DMSO/PBS (7:3, v/v) following the addition of different analytes. **(d)** Fluorescence variations of probe PH-Cys under excitation with a 365 nm UV lamp, after the addition of different analytes.

Figure S23. (a) Temporal variations in the fluorescence intensity of probe PH-Cys (10.0 μM) at 779 nm in DMSO/PBS (7:3, v/v), recorded in the absence and presence of cysteine (Cys; 6.0 μM and 12.0 μM). **(b)** Fluorescence intensity of probe PH-Cys (10.0 μM) at 779 nm across a pH range of 2.0-12.0 in DMSO/PBS (7:3, v/v), measured both prior to and following Cys supplementation.

Figure S24. The particle size of probe PH-Cys (10.0 μM) following the addition of Cys in DMSO/PBS (7:3, v/v) was measured at **(a)** pH = 7.4 and **(b)** pH = 12.

Figure S25. (a) Results of the PH-Cys and Cys reaction process monitored by HPLC. **(b)** Frontier molecular orbitals of PH-Cys and PH-OH.

Figure. S26. Mass spectrum of PH-Cys and the addition of Cys.

Figure S27. Diagram illustrating the determination of RGB values of solution color via smartphone-based measurement, depicting the color variation of PH-Cys probe with the change of Cys concentration in the range of 0 μM to 12.0 μM, as well as the linear correlation between the R+G/B ratio (R, G, B represent red, green, blue channels respectively) and Cys concentration within the range of 0 μM to 12.0 μM.

Figure S28. (a) Detection of Cys in real samples. **(b)** Changes in fluorescence intensity of probe PH-Cys upon the addition of Cys at different concentrations in actual samples.

Figure S29. Cytotoxicity of probe PH-Cys.

Figure S30. Confocal laser scanning microscopy (CLSM) images of cells stained with probe PH-Cys (10.0 μM). **(a)** Brightfield image of RAW 264.7 cells co-stained with PH-Cys alone; **(b)** Fluorescence image of the cells in **(a)** acquired under the red channel; **(c)** Merged image of **(a)** and **(b)**. **(d)** Brightfield image of RAW 264.7 cells co-stained with PH-Cys and pretreated with N-ethylmaleimide (NEM); **(e)** Fluorescence image of the cells in **(d)** acquired under the red channel; **(f)** Merged image of **(d)** and **(e)**. **(g)** Brightfield image of RAW 264.7 cells co-stained with PH-Cys, pretreated with NEM, and subsequently treated with 4.0 μM cysteine (Cys); **(h)** Fluorescence image of the cells in **(g)** acquired under the red channel; **(i)** Merged image of **(g)** and **(h)**. **(j)** Brightfield image of RAW 264.7 cells co-stained with PH-Cys, pretreated with NEM, and subsequently treated with 8.0 μM Cys; **(k)** Fluorescence image of the cells in **(j)** acquired under the red channel; **(l)** Merged image of **(j)** and **(k)**. **(m)** Brightfield image of RAW 264.7 cells co-stained with PH-Cys, pretreated with NEM, and subsequently treated with 12.0 μM Cys; **(n)** Fluorescence image of the cells in **(m)** acquired under the red channel; **(o)** Merged image of **(m)** and **(n)**. (Excitation wavelength, λ_{ex} = 561 nm; Emission wavelength range, λ_{em} = 650-750 nm; Scale bar: 10 μm.)

Figure S31. Confocal laser scanning microscopy (CLSM) images of zebrafish stained with probe PH-Cys (10.0 μM). **(a)** Brightfield image of zebrafish co-stained with PH-Cys alone; **(b)** Fluorescence image of the zebrafish in **(a)** acquired under the red channel; **(c)** Merged image of **(a)** and **(b)**. **(d)** Brightfield image of zebrafish co-stained with PH-Cys and pretreated with N-ethylmaleimide (NEM); **(e)** Fluorescence image of the zebrafish in **(d)** acquired under the red channel; **(f)** Merged image of **(d)** and **(e)**. **(g)** Brightfield image of zebrafish co-stained with PH-Cys, pretreated with NEM, and subsequently treated with 4.0 μM cysteine (Cys); **(h)** Fluorescence image of the

zebrafish in **(g)** acquired under the red channel; **(i)** Merged image of **(g)** and **(h)**. **(j)** Brightfield image of zebrafish co-stained with PH-Cys, pretreated with NEM, and subsequently treated with 8.0 μM Cys; **(k)** Fluorescence image of the zebrafish in **(j)** acquired under the red channel; **(l)** Merged image of **(j)** and **(k)**. **(m)** Brightfield image of zebrafish co-stained with PH-Cys, pretreated with NEM, and subsequently treated with 12.0 μM Cys; **(n)** Fluorescence image of the zebrafish in **(m)** acquired under the red channel; **(o)** Merged image of **(m)** and **(n)**. (Excitation wavelength, λ_{ex} = 561 nm; Emission wavelength range, λ_{em} = 650-750 nm; Scale bar: 500 μm.)

Figure S32. (a) Average fluorescence intensity in the red channel of confocal laser scanning microscopy (CLSM) images of RAW 264.7 cells. **(b)** Average fluorescence intensity in the red channel of confocal laser scanning microscopy (CLSM) images of zebrafish.

Table S1. Determination of Cys concentration in different samples.

Table S2. Comparison of properties of PH-Cys with reported Cys fluorescent probes.

All reagents and chemicals were obtained from Energy Chemical and used without further purification unless otherwise stated. Column chromatography silica gel was bought from Yantai Xinnuo Chemical Co., Ltd. NMR spectra were obtained on Bruker 400 M spectrometers. High-resolution mass spectra (HRMS) were measured with a Waters XEVO-G2-QTOF. The high performance liquid chromatography utilizes an Agilent 1260 system. UV/Vis spectra were recorded on a Hitachi UV-3310 UV/Vis

spectrometer. Fluorescence data were recorded on an FLS1000 spectrofluorometer (Edinburgh, Britain). Cell and zebrafish imaging was performed on a Nikon Confocal (Japan).

1.1. Synthesis of Compound 1

Under nitrogen protection, add 1.5 mL (12.22 mmol) of benzyl propargyl aldehyde and 36.6 mL (18.33 mmol) of 1-propargyl magnesium bromide to 15.0 mL of anhydrous THF solution. Stir at -20°C for 20 min, then raise to room temperature and react for 2 h. After the reaction, TLC was used to monitor the progress. The reaction was quenched by adding saturated ammonium chloride solution until no more bubbles were observed in the reaction mixture. The reaction mixture was then extracted with DCM (3 × 30.0 mL), washed with distilled water, dried over anhydrous $MgSO_4$, and filtered under vacuum to obtain the organic phase. The solvent was removed from the organic phase by rotary evaporation. The crude product was purified on a silica gel column (PE: EA = 8: 1) to obtain a yellow oily compound **1** (1.4 g, 70%). ^{1}H NMR (400 MHz, Chloroform-*d*) δ 7.44 (dd, *J* = 7.7, 1.9 Hz, 2H), 7.28 - 7.21 (m, 3H), 5.37 (d, *J* = 2.2 Hz, 1H), 3.74 (s, 1H), 1.82 (d, *J* = 2.3 Hz, 3H). ^{13}C NMR (100 MHz, Chloroform-*d*) δ 131.84, 128.69, 128.28, 122.13, 86.89, 83.74, 81.33, 76.84, 52.56, 3.65. HRMS (ESI) m/z: $[M+H]^+$ calcd for $C_{12}H_{11}O$: 171.0804, found: 171.0858.

1.2. Synthesis of Compound 2

Compound **1** (1.5 g, 8.52 mmol) was dissolved in 20.0 mL of dichloromethane along with manganese dioxide (14.8 g, 170.38 mmol), and the mixture was stirred at room temperature for 12 h. After the reaction was complete, TLC was used to monitor the progress. The solution was filtered through diatomaceous earth until clear, and the organic phase was evaporated under reduced pressure to obtain the white solid compound **2** (1.2 g, 82%). ^{1}H NMR (400 MHz, Chloroform-*d*) δ 7.65 - 7.56 (m, 2H),

7.50 - 7.45 (m, 1H), 7.39 (t, *J* = 7.5 Hz, 2H), 2.10 (s, 3H). ^{13}C NMR (100 MHz, Chloroform-*d*) δ 161.09, 133.32, 131.14, 128.68, 119.50, 91.73, 90.60, 89.29, 81.52, 4.44. HRMS (ESI) m/z: $[M+H]^+$ calcd for $C_{12}H_9O$: 169.0648, found: 169.0683.

1.3. Synthesis of Compound 3

Under nitrogen protection, compound **2** (1.4 g, 8.50 mmol) was dissolved in 20.0 mL of anhydrous DMF with thiourea (666.6 mg, 8.76 mmol) and stirred at room temperature for 14 h. TLC analysis. After the reaction was complete, the reaction mixture was poured into ice water, extracted with DCM (3 × 30.0 mL), washed with distilled water, dried with anhydrous $MgSO_4$, and filtered under vacuum to obtain the organic phase. The solvent was removed from the organic phase by rotary evaporation. The crude product was purified on a silica gel column (PE: EA = 1: 1), yielding a brownish-yellow oily compound **3** (1.1 g, 66%). ^{1}H NMR (400 MHz, Chloroform-*d*) δ 7.57 (dd, *J* = 7.4, 2.1 Hz, 2H), 7.51 - 7.43 (m, 3H), 7.13 (s, 1H), 6.86 (s, 1H), 2.45 (s, 3H). ^{13}C NMR (100 MHz, Chloroform-*d*) δ 182.32, 153.28, 151.29, 135.93, 130.68, 129.32, 128.42, 126.77, 126.68, 22.78. HRMS (ESI) m/z: $[M+H]^+$ calcd for $C_{12}H_{11}OS$: 203.0525, found: 203.0559.

1.4. Synthesis of Compound 4

Compound **3** (1.1 g, 5.64 mmol) and propionitrile (3.7 g, 56.36 mmol) were dissolved in 25.0 mL of acetic anhydride. The mixture was refluxed at 140°C for 4 h. After TLC analysis confirmed complete reaction, the temperature was lowered to 90°C, and 55.0 mL of methanol was added to the reaction mixture. The mixture was quenched at 90°C for 30 min. After quenching, the reaction mixture was cooled to room temperature, extracted with DCM (3 × 60.0 mL), washed with distilled water, dried over anhydrous $MgSO_4$, and filtered under vacuum to obtain the organic phase. The solvent was removed from the organic phase by rotary evaporation. The crude product

was purified using a silica gel column (PE : EA = 8 : 1), yielding a yellow solid **4** (650.0 mg, 46%). ^{1}H NMR (400 MHz, Chloroform-*d*) δ 7.62 - 7.58 (m, 2H), 7.55 - 7.51 (m, 3H), 7.50 (d, *J* = 1.5 Hz, 1H), 7.30 - 7.27 (m, 1H), 2.53 (s, 3H). ^{13}C NMR (100 MHz, Chloroform-*d*) δ 156.94, 152.56, 150.54, 135.11, 131.53, 129.62, 126.92, 121.59, 120.31, 108.88, 64.87, 23.10. HRMS (ESI) m/z: $[M-H]^-$ calcd for $C_{15}H_9N_2S$: 249.0492, found: 249.0533.

1.5. Synthesis of Compound PH-OH

Under nitrogen protection, dissolve compound **4** (80.0 mg, 319.59 μmol) and compound **5** (50.6 mg, 266.33 μmol) in 10.0 mL of anhydrous ethanol, mix thoroughly, then add 0.1 mL of piperidine and 0.1 mL of acetic acid to the system. Reflux the mixture at 85°C for 12 h. After TLC detection, the reaction mixture was dried under reduced pressure, recrystallized, and yielded a dark red powder compound PH-OH (46.2 mg, 41%). ^{1}H NMR (400 MHz, DMSO-d_6) δ 8.40 (s, 1H), 7.82 - 7.76 (m, 3H), 7.65 - 7.61 (m, 2H), 7.60 (d, *J* = 6.3 Hz, 1H), 7.52 (d, *J* = 8.7 Hz, 1H), 7.41 (s, 1H), 7.39 - 7.31 (m, 2H), 6.82 (dd, *J* = 8.6, 2.1 Hz, 1H), 6.70 (d, *J* = 1.9 Hz, 1H). ^{13}C NMR (100 MHz, DMSO-d_6) δ 182.68, 171.74, 164.95, 159.90, 159.86, 156.45, 153.63, 153.46, 149.97, 144.13, 143.81, 135.39, 132.23, 131.21, 130.24, 127.42, 126.85, 121.90, 117.03, 116.63, 115.84, 72.31. HRMS (ESI) m/z: $[M-H]^-$ calcd for $C_{25}H_{13}N_2O_3S$: 421.0652, found: 421.0651.

1.6. Synthesis of Compound PH-Cys

Compound PH-OH (46.0 mg, 108.89 μmol) was dissolved in dry DCM (5.0 mL) under nitrogen protection. Triethylamine (60.4 μL, 435.55 μmol) and acryloyl chloride (49.7 mL, 653.32 μmol) were added dropwise. The reaction was conducted at ambient temperature for a duration of 2.0 h. The reaction completion should be monitored via thin-layer chromatography. The mixture should then be dried under reduced pressure.

After recrystallization, an orange-red solid compound PH-Cys (31.0 mg, 60%) was obtained. ^{1}H NMR (400 MHz, DMSO-d_6) δ 8.76 (d, J = 36.2 Hz, 1H), 8.61 (s, 1H), 8.49 - 8.31 (m, 1H), 8.04 (dd, J = 19.5, 8.2 Hz, 1H), 7.81 (s, 1H), 7.61 (s, 1H), 7.50 (d, J = 8.6 Hz, 1H), 7.39 (s, 1H), 7.30 (d, J = 18.1 Hz, 2H), 6.60 (d, J = 16.8 Hz, 2H), 6.45 (dd, J = 17.0, 10.7 Hz, 2H), 6.23 (d, J = 8.6 Hz, 2H). ^{13}C NMR (150 MHz, DMSO-d_6) δ 188.44, 164.03, 159.42, 155.50, 155.01, 154.44, 154.31, 153.06, 148.22, 146.74, 146.62, 135.14, 134.85, 132.95, 132.24, 130.26, 127.75, 127.63, 126.58, 119.28, 111.25, 106.77, 93.19, 85.66. HRMS (ESI m/z): $[M+H]^+$ calcd for $C_{28}H_{17}N_2O_4S$: 477.0904, found: 477.0907.

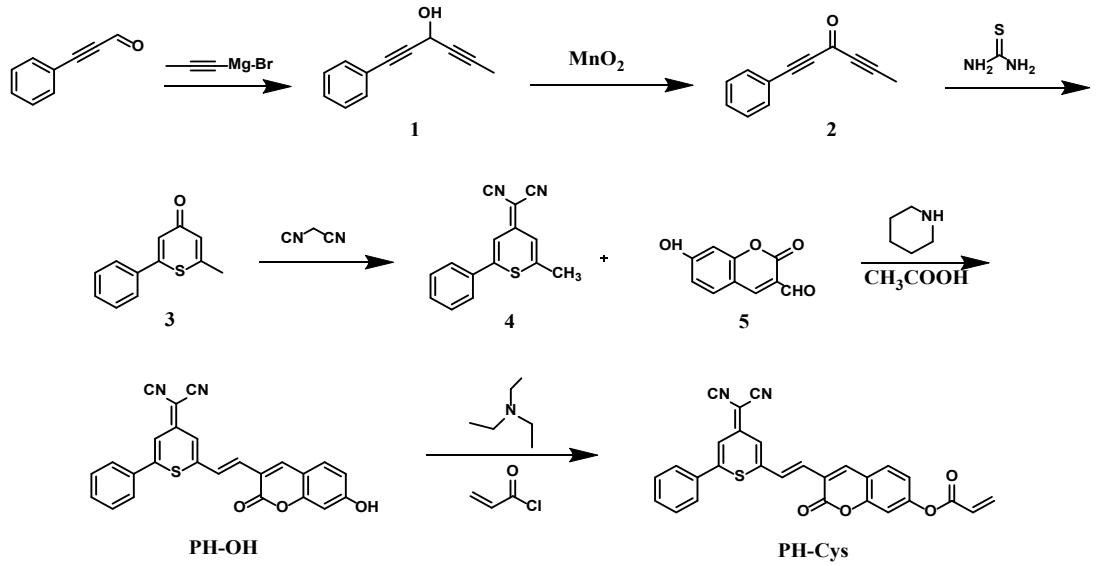

Scheme S1. The synthetic route of probe PH-Cys.

2.1. Spectral testing conditions

The probe PH-Cys was accurately weighed and dissolved in analytical-grade DMSO to prepare a probe stock solution (10 mL, 1 mM), which was stored at a low temperature (4 °C) in the dark. Take 20 μL of the probe stock solution and dilute it to a final concentration of 10.0 μM (10 mM, pH = 7.4) using a buffer solution made with a 7:3 volume ratio of DMSO and PBS. The solution was then analyzed using UV

fluorescence spectroscopy. Meanwhile, the control amino acid samples were prepared as 1 mM solutions in deionized water for specificity experiments.

2.2. Preparation of samples

This study employed six samples: pear, peach, strawberry, orange, cabbage, and bean. All samples were procured from local markets and tested in their fresh state. Following homogenisation, samples were centrifuged at 5000 $r \cdot min^{-1}$ to obtain supernatant. This was diluted 100-fold with PBS buffer (pH=7.4), then sequentially supplemented with cystine solutions at concentrations of 0 μM, 0.5 μM, 3.0 μM, 5.0 μM, 8.0 μM, and 10.0 μM. followed by the addition of the fluorescent probe (final concentration 10.0 μM) for a 20.0 min reaction period prior to fluorescence detection. Experiments were replicated to record data and calculate the relative standard deviation (RSD).

2.3. Cytotoxicity assay

Toxicity studies and biological imaging of cells and living organisms are crucial applications of fluorescent probes. The first step is to test the cytotoxicity of the probe PH-Cys. A certain number of RAW 264.7 cells were cultured in a 96-well plate for 24.0 h in an incubator, allowing the cells to adhere to the walls of the plate. The cells were then treated with different concentrations (2.5 μM, 5.0 μM, 10.0 μM, 15.0 μM, and 20.0 μM) of the probe PH-Cys for 48.0 h to allow the probe to enter the cells. Afterward, the cells were washed with PBS and the Cell Counting Kit-8 reagent was added. The cells were further cultured for 30.0 min in the incubator, and the cytotoxicity was assessed using a microplate reader.

2.4. Confocal imaging experiments on cells and zebrafish

RAW 264.7 cells were seeded into five confocal culture dishes and cultured at 37 °C in a cell culture incubator containing 5% carbon dioxide for 24.0 h to allow them to adhere to the dish walls. Subsequently, four of the dishes were treated with 50 nM NEM for 1.0 h to remove endogenous cysteine from the cells. The five groups of cells were then incubated with PH-Cys (10.0 μM) for 30.0 min. After incubation, the excess probe solution was washed off with PBS. Three of the dishes that had been treated with NEM and lacked endogenous cysteine were selected. These three dishes were then supplemented with cysteine solutions (4.0 μM, 8.0 μM, and 12.0 μM) and continued to be cultured for 30.0 min. Subsequently, imaging of the five groups of cells was performed using a laser confocal microscope (The cell density of RAW 264.7 cells employed for imaging experiments was 18.67×10^6 cells/mL).

Five groups of zebrafish were cultured in deionized water. The first group served as the control group, incubated with 10.0 μM PH-Cys probe solution for 30.0 min, washed to remove excess probe solution, anesthetized, and imaged using a laser confocal microscope. The second group was pretreated with NEM for 1.0 h to remove intracellular Cys, washed to remove excess NEM, then incubated with 10.0 μM PH-Cys probe solution for 30.0 min, washed to remove excess probe solution, anesthetized, and imaged using a laser confocal microscope. Groups 3 to 5 were based on Group 2, with exogenous cysteine solutions (4.0 μM, 8.0 μM, 12.0 μM) added and incubated for 30.0 min. After washing, anesthesia was administered, and imaging was performed using a laser confocal microscope.

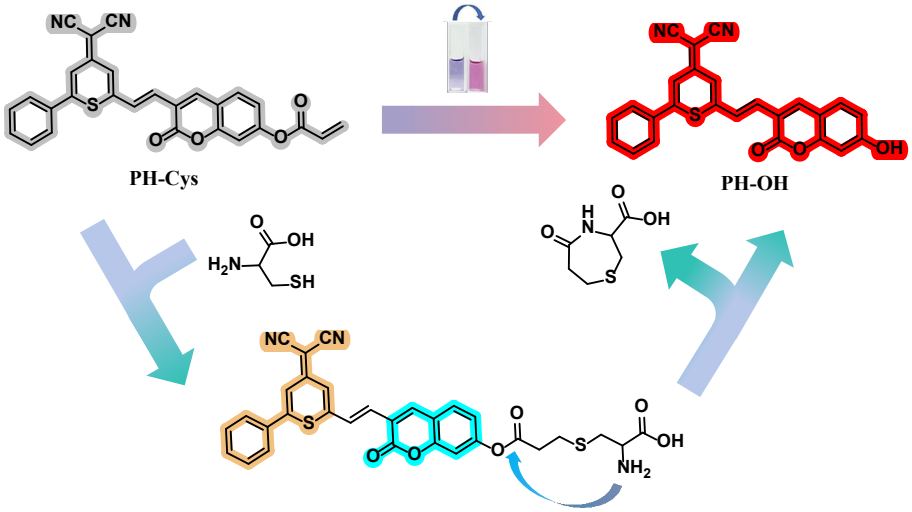

Scheme S2. The reaction mechanism of PH-Cys with Cys.

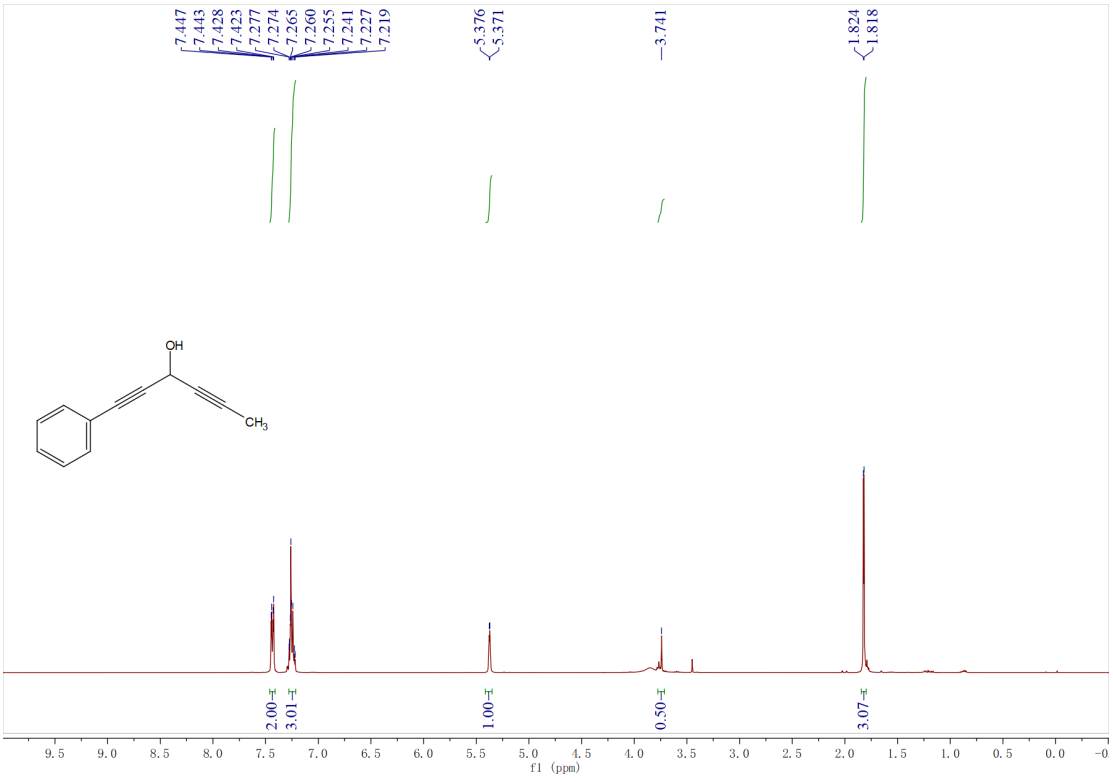

Figure S1. ^{1}H NMR (400 MHz, $CDCl_3$) spectra of compound **1**.

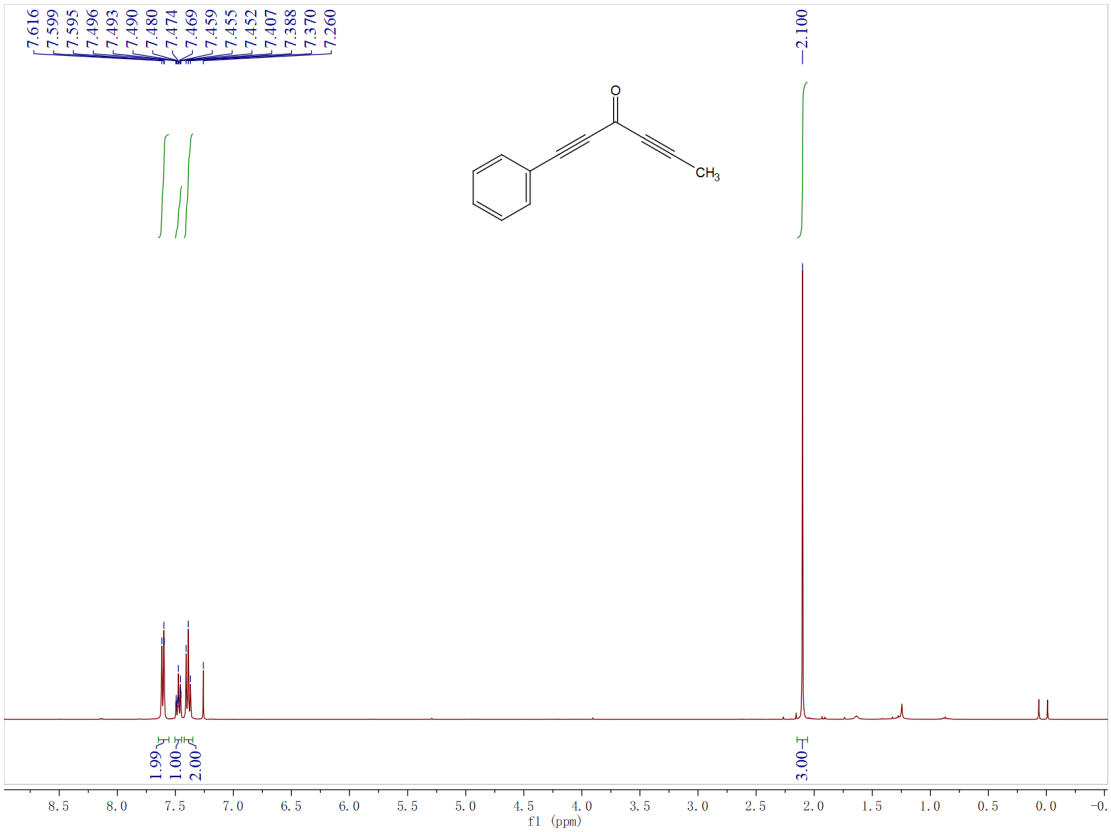

Figure S2. ^{1}H NMR (400 MHz, $CDCl_3$) spectra of compound **2**.

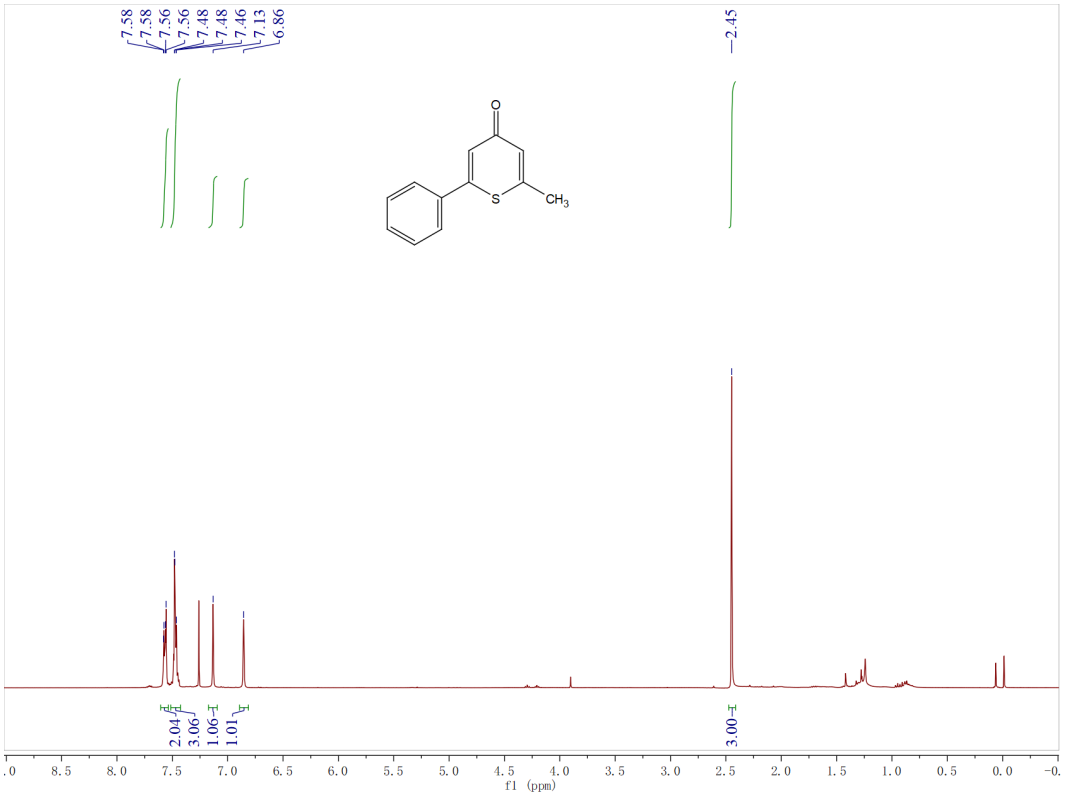

Figure S3. ^{1}H NMR (400 MHz, $CDCl_3$) spectra of compound **3**.

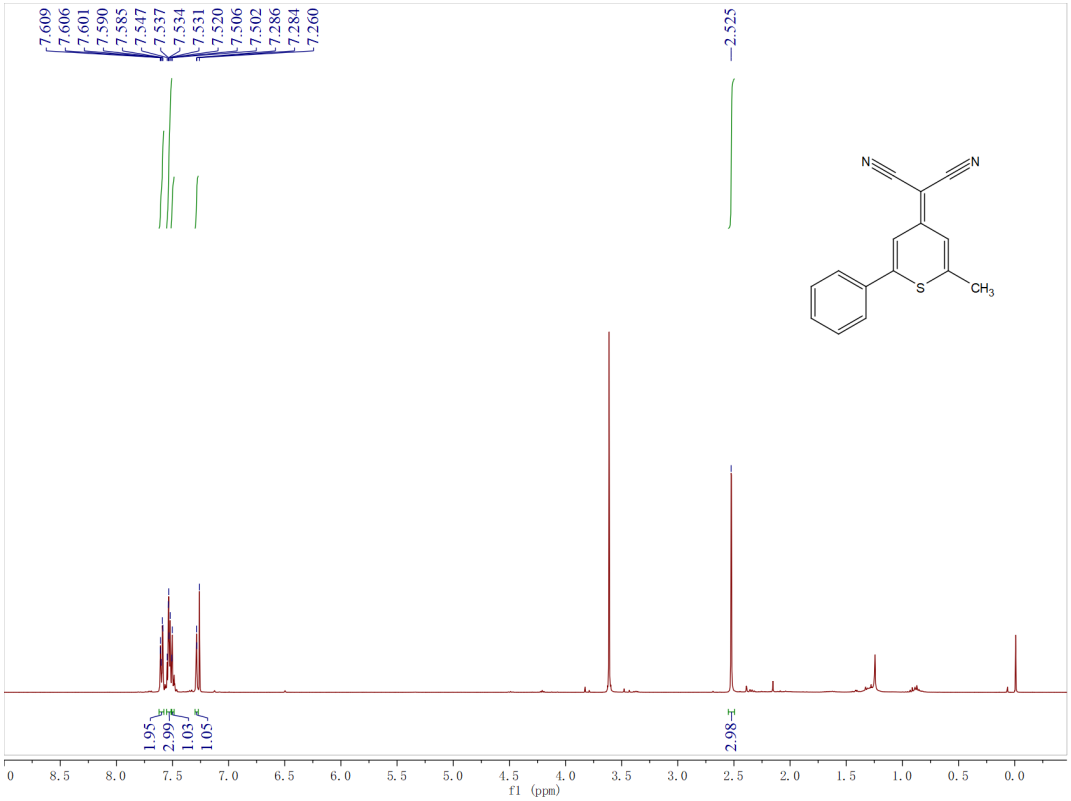

Figure S4. ^{1}H NMR (400 MHz, $CDCl_3$) spectra of compound **4**.

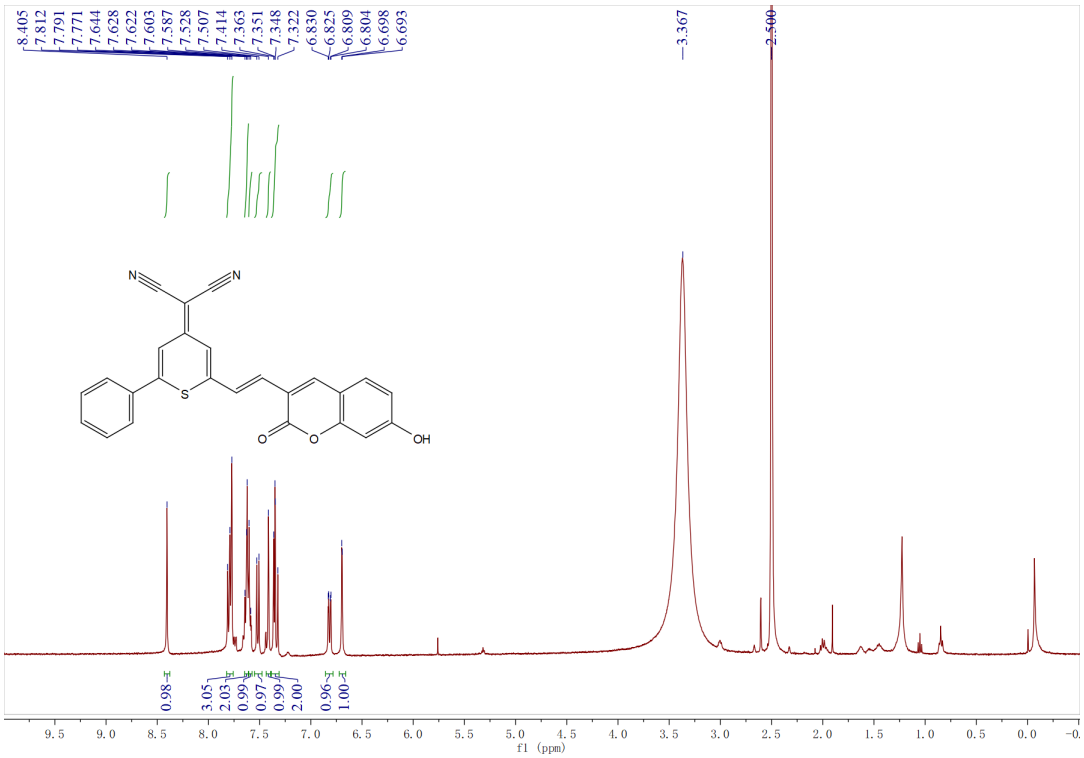

Figure S5. ^{1}H NMR (400 MHz, DMSO-d_6) spectra of PH-OH.

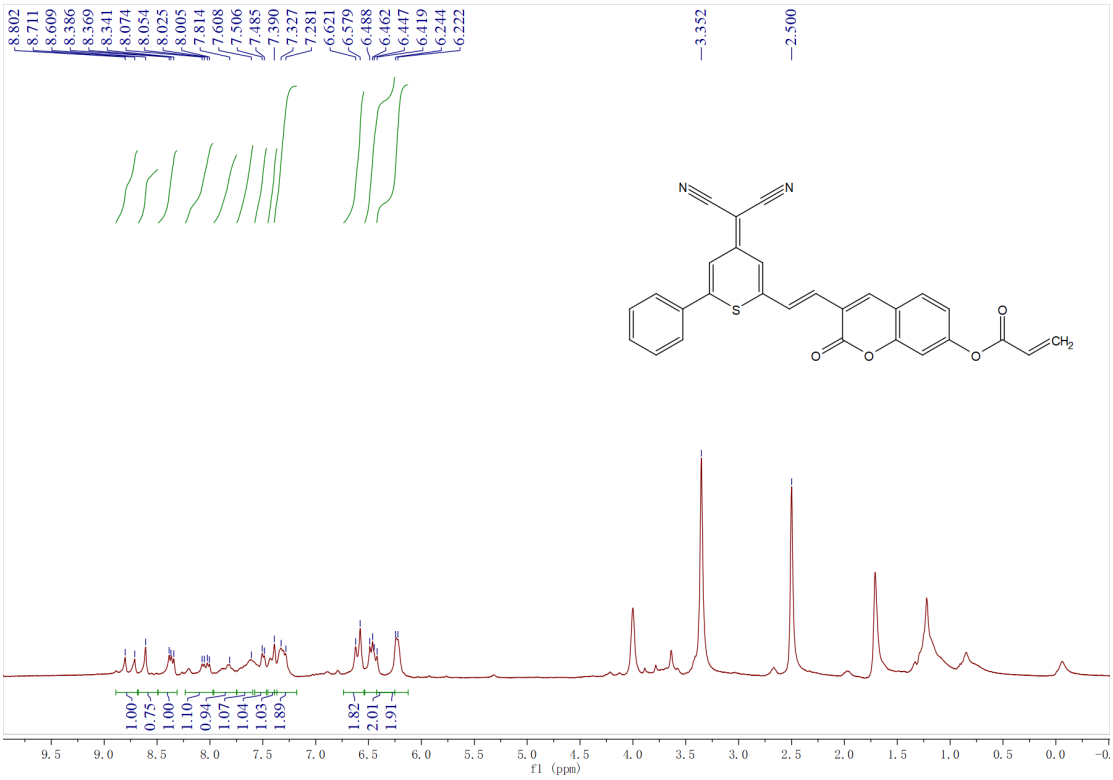

Figure S6. ^{1}H NMR (400 MHz, DMSO-d_6) spectra of compound PH-Cys.

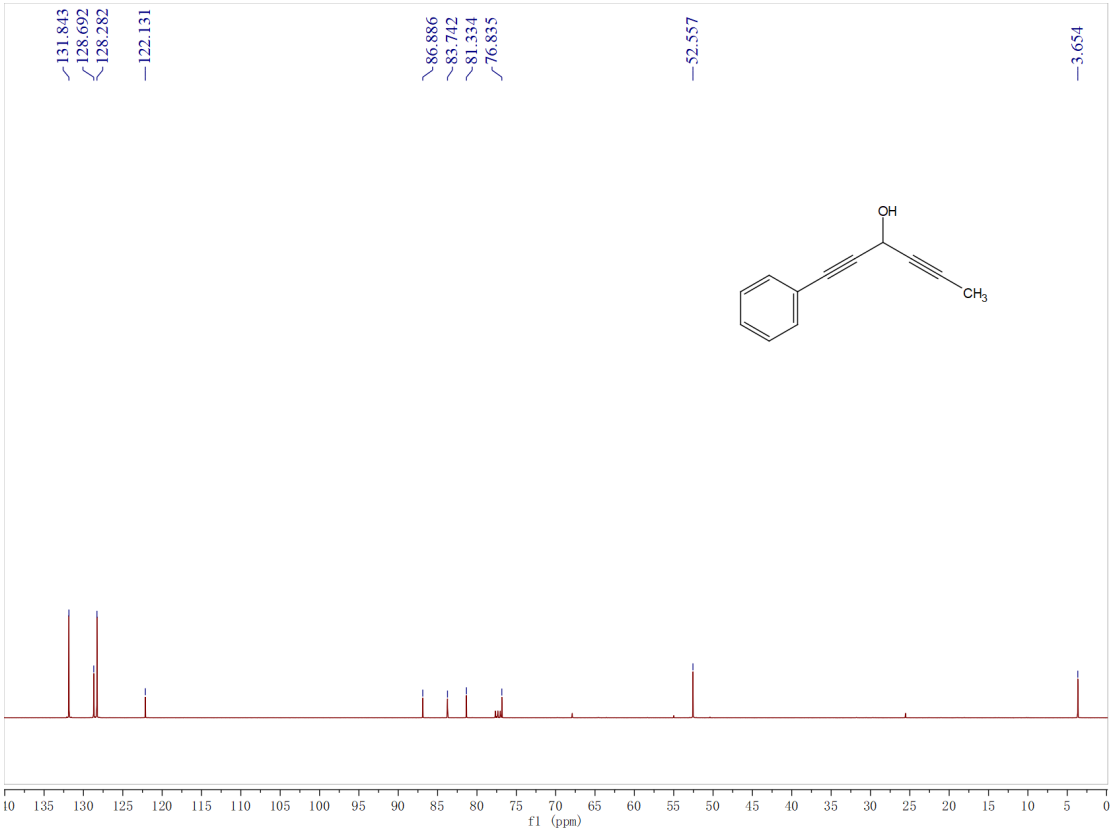

Figure S7. ^{13}C NMR (100 MHz, $CDCl_3$) spectra of compound **1**.

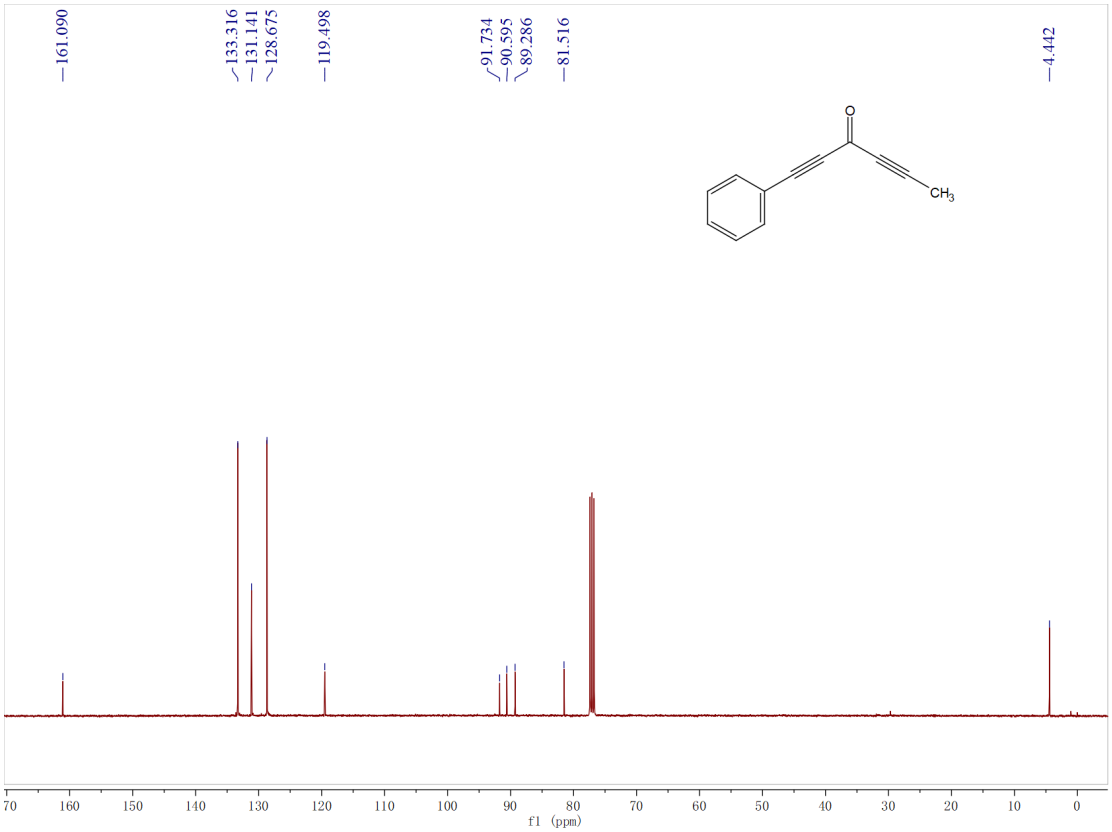

Figure S8. ^{13}C NMR (100 MHz, $CDCl_3$) spectra of compound **2**.

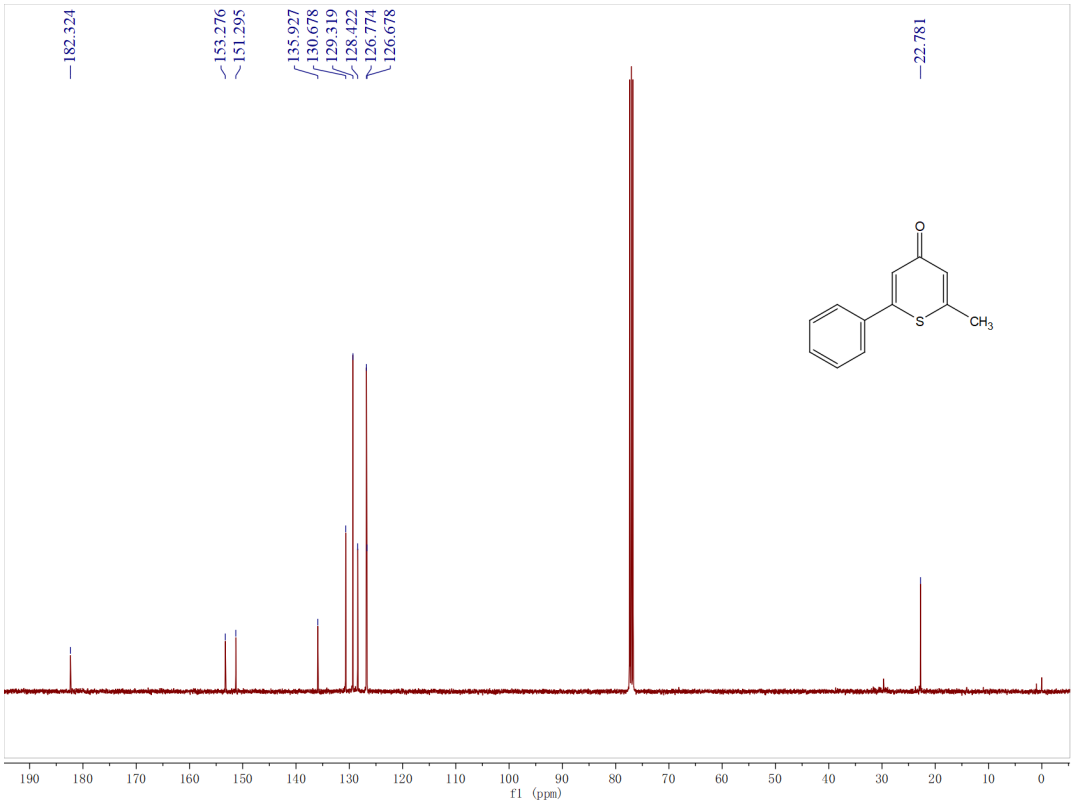

Figure S9. ^{13}C NMR (100 MHz, $CDCl_3$) spectra of compound **3**.

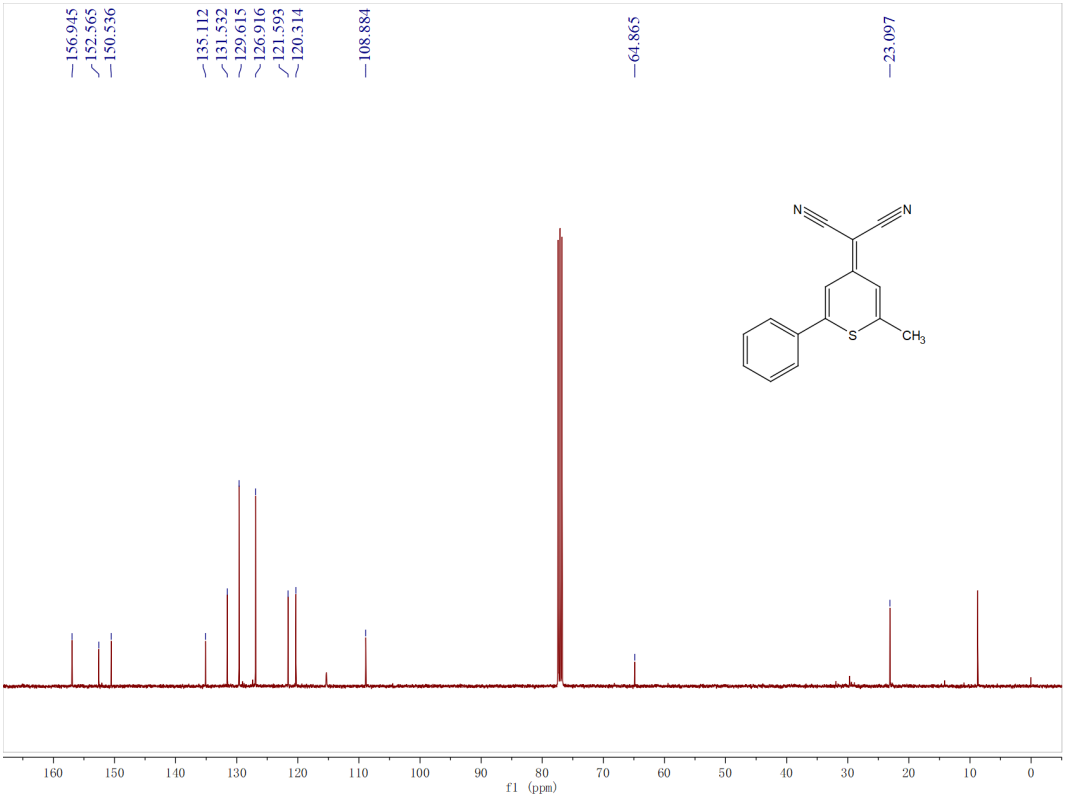

Figure S10. ^{13}C NMR (100 MHz, $CDCl_3$) spectra of compound **4**.

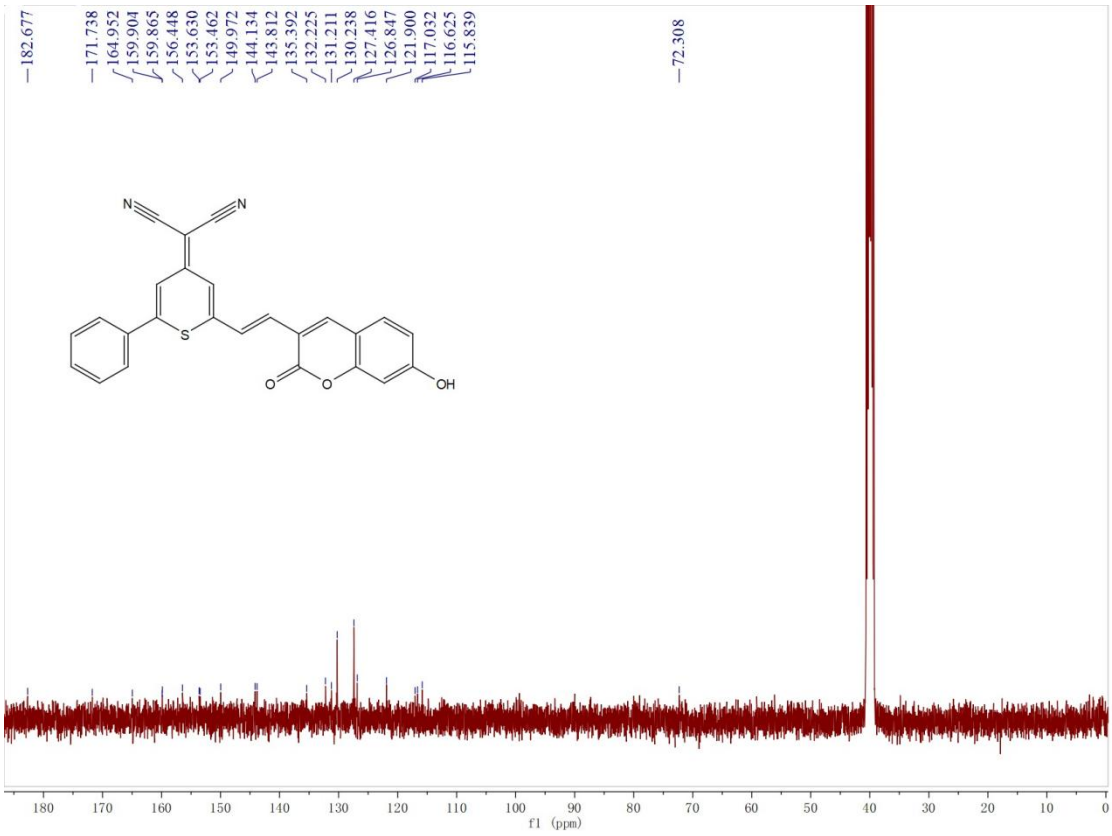

Figure S11. ^{13}C NMR (100 MHz, DMSO-d_6) spectra of PH-OH.

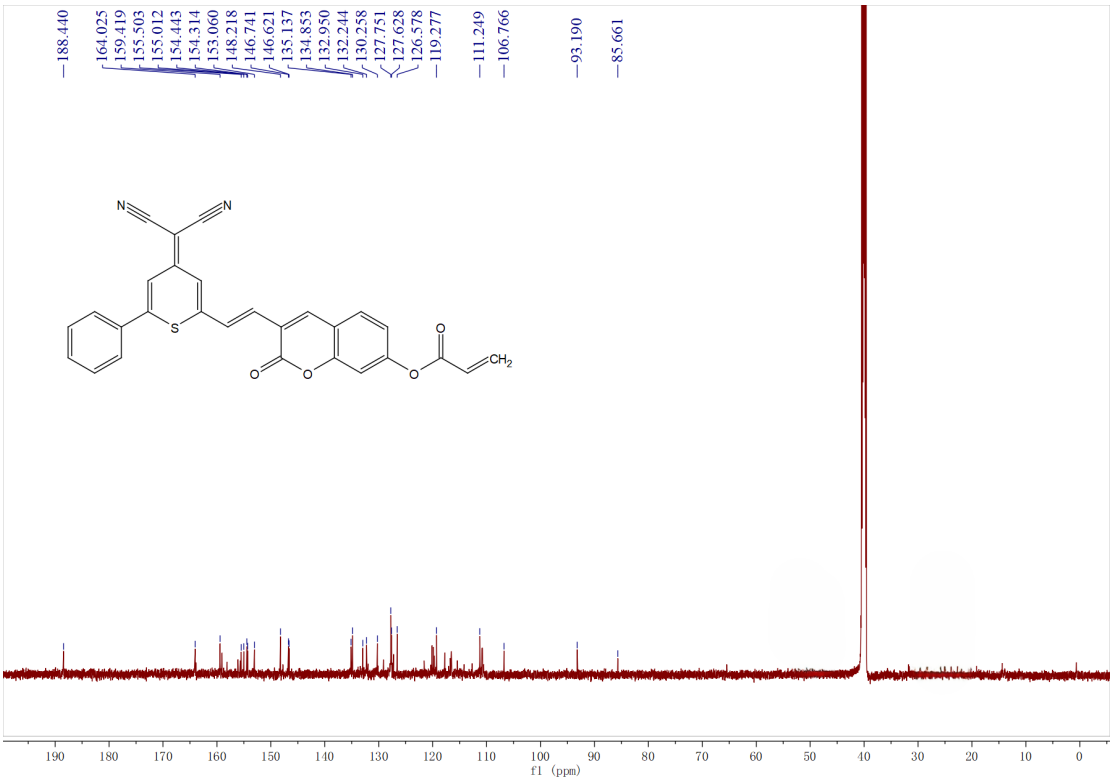

Figure S12. ^{13}C NMR (150 MHz, DMSO-d_6) spectra of PH-Cys.

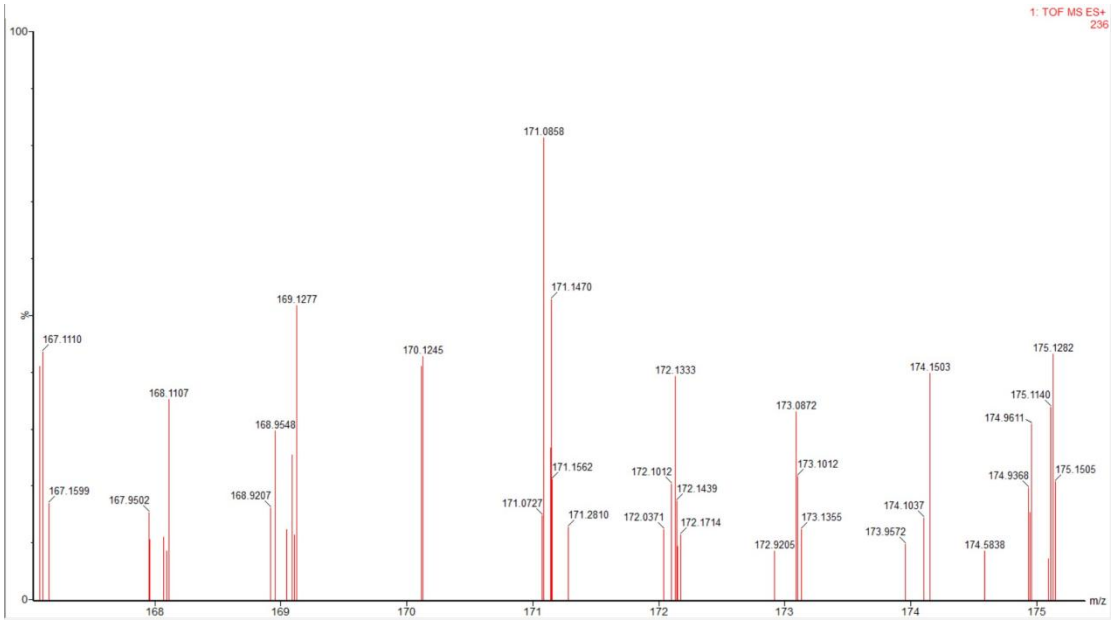

Figure S13. TOF-MS spectra of compound **1**.

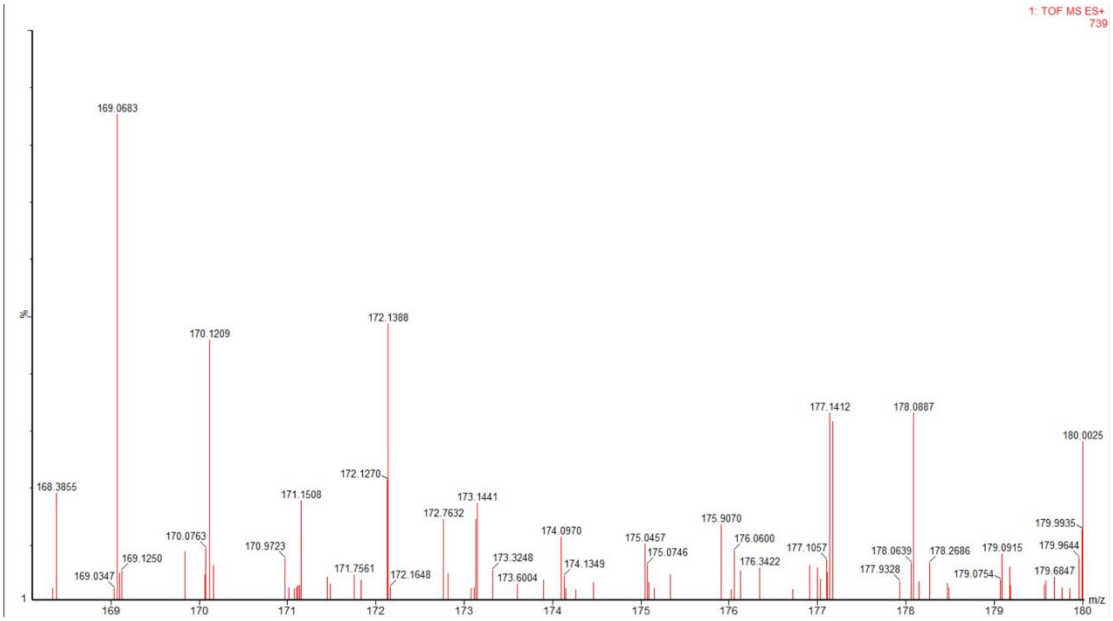

Figure S14. TOF-MS spectra of compound **2**.

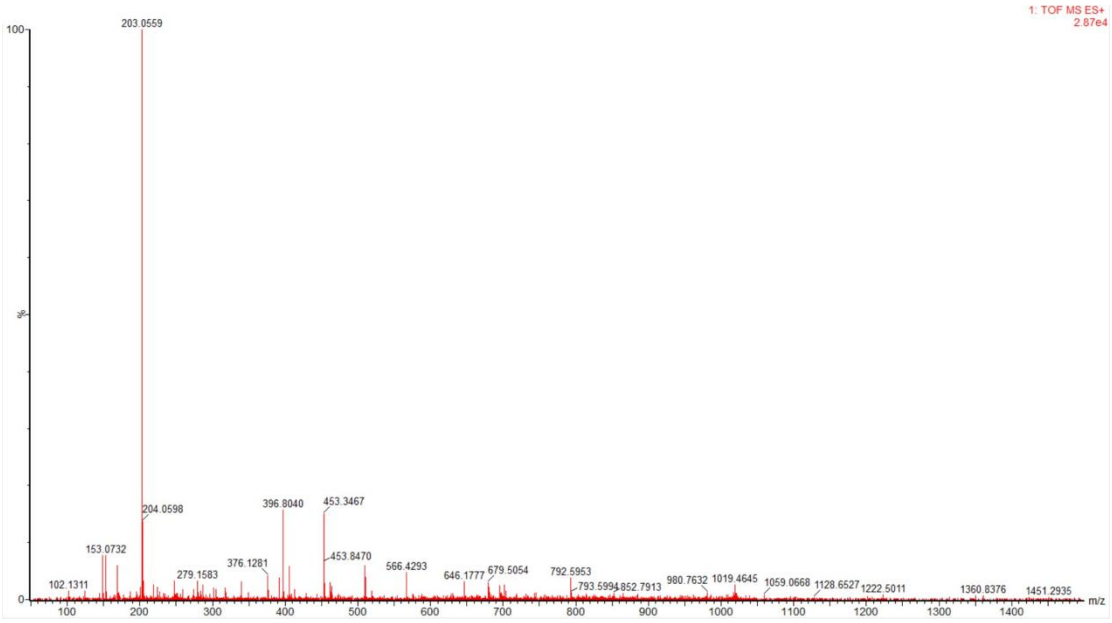

Figure S15. TOF-MS spectra of compound **3**.

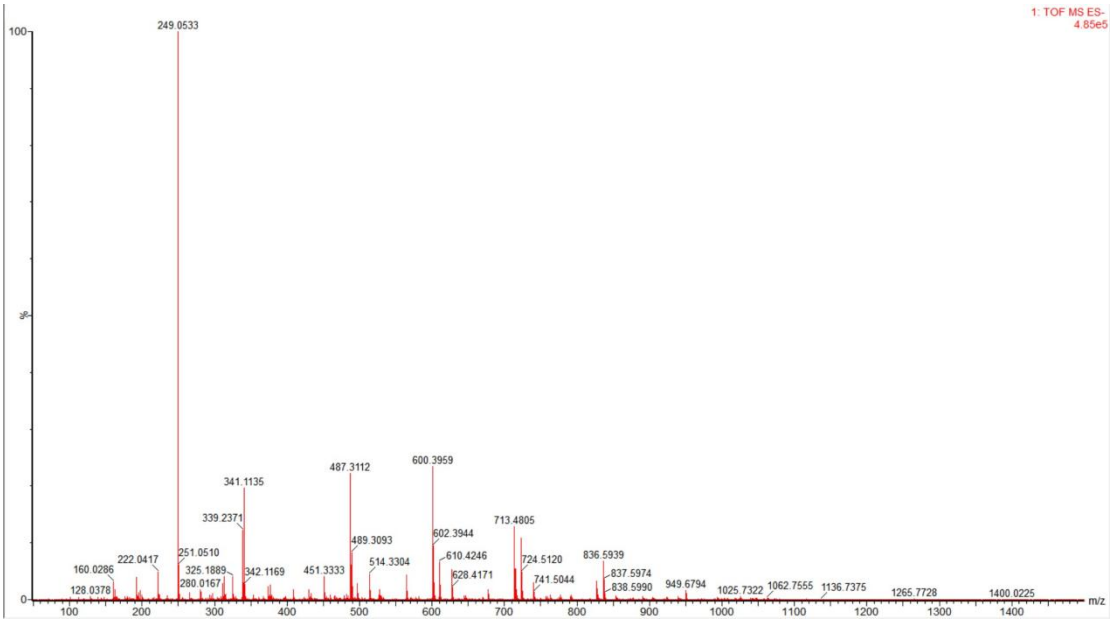

Figure S16. TOF-MS spectra of compound **4**.

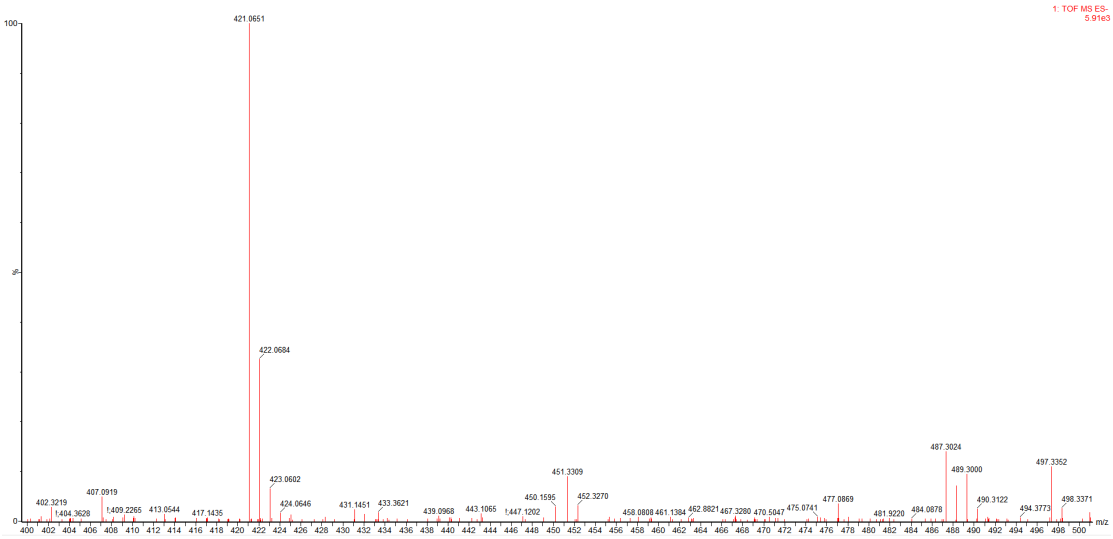

Figure S17. TOF-MS spectra of PH-OH.

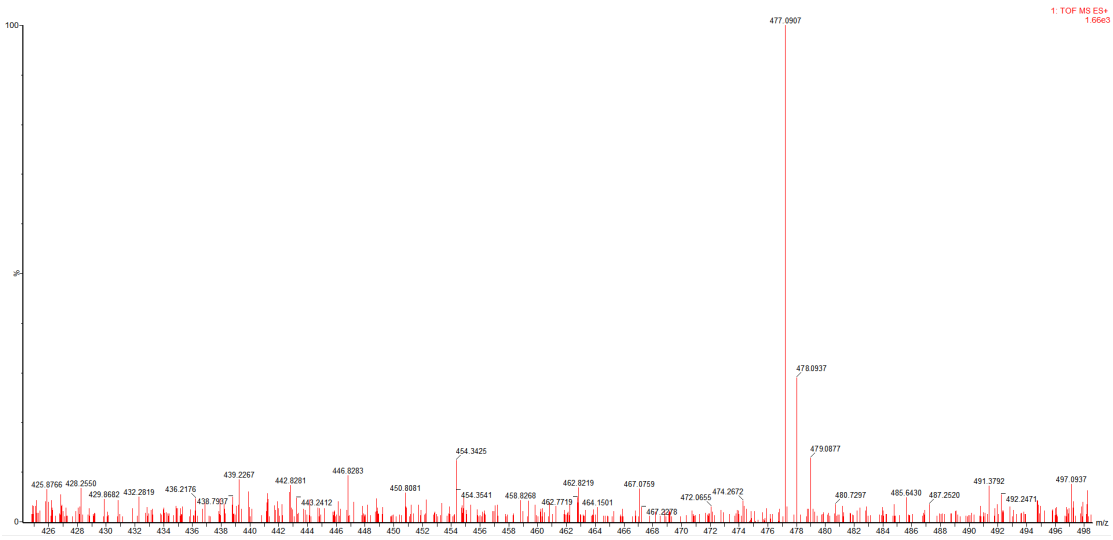

Figure S18. TOF-MS spectra of PH-Cys.

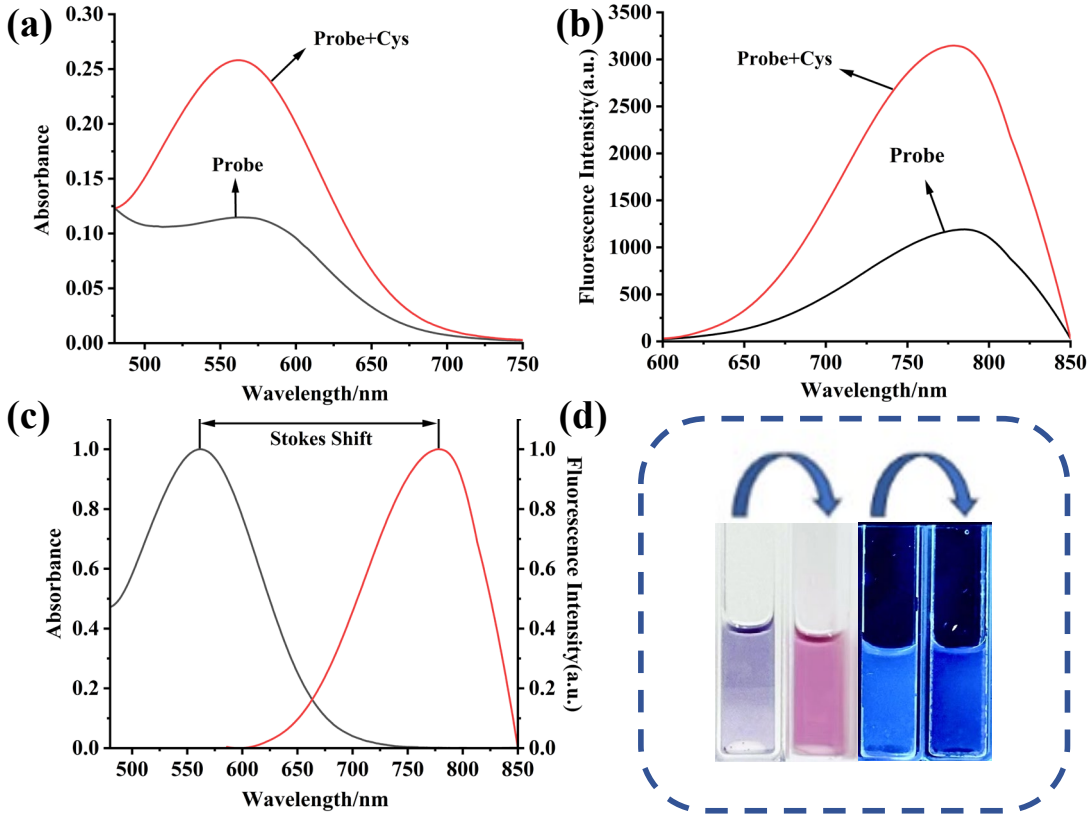

Figure S19. (a) UV-vis absorption spectral and **(b)** fluorescence emission spectral responses of probe PH-Cys towards Cys. **(c)** Normalized Stokes shift diagram of probe PH-Cys (Stokes shift = 217 nm). **(d)** Color variations of PH-Cys upon Cys addition, and fluorescence variations of PH-Cys upon Cys addition under excitation with a 365

nm UV lamp.

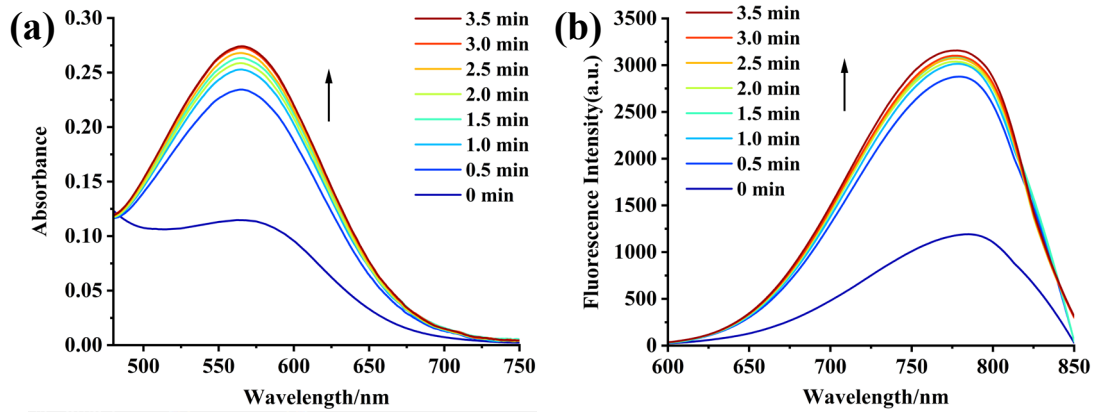

Figure S20. (a) UV-vis absorption spectra and **(b)** fluorescence emission spectra for the time-dependent response of probe PH-Cys towards Cys.

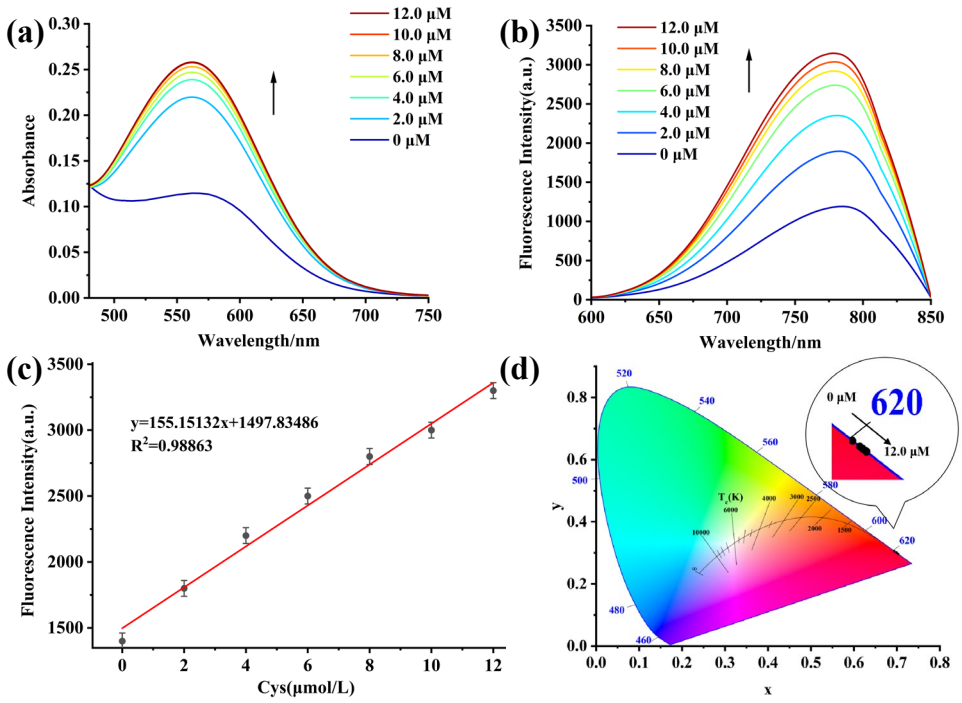

Figure S21. (a) UV-vis absorption spectra of probe PH-Cys and **(b)** fluorescence emission spectra of probe PH-Cys for the concentration-dependent response towards Cys. **(c)** Linear relationship between probe PH-Cys and Cys concentration. **(d)** CIE 1931 chromaticity coordinates (x, y) of probe PH-Cys at varying Cys concentrations.

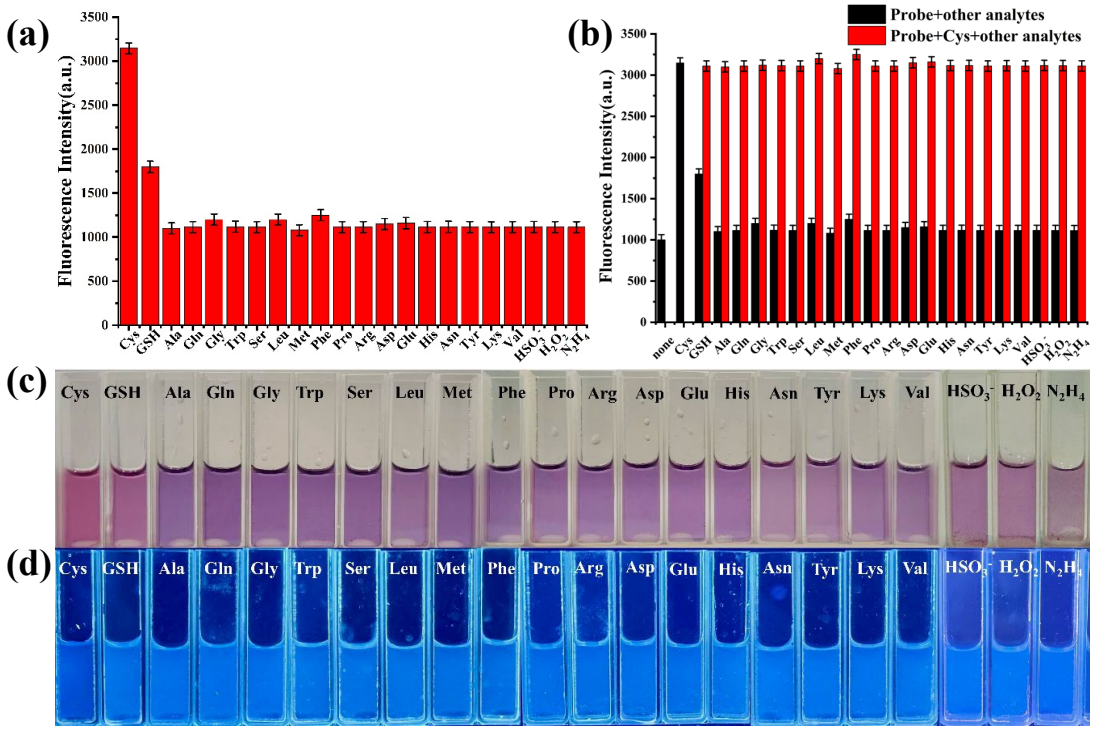

Figure S22. (a) Fluorescence intensity at 779 nm of probe PH-Cys (10.0 μM) in the presence of various analytes in DMSO/PBS (7:3, v/v) at ambient temperature (all analytes were used at a concentration of 12.0 μM). **(b)** Fluorescence responses of probe PH-Cys (10.0 μM) towards various analytes. Black bars correspond to the addition of different analytes (12.0 μM) to the PH-Cys (10.0 μM) solution; red bars correspond to the subsequent addition of cysteine (Cys) and other analytes (12.0 μM) to the aforementioned solution. **(c)** Color of the PH-Cys solution in DMSO/PBS (7:3, v/v) following the addition of different analytes. **(d)** Fluorescence variations of probe PH-Cys under excitation with a 365 nm UV lamp, after the addition of different analytes.

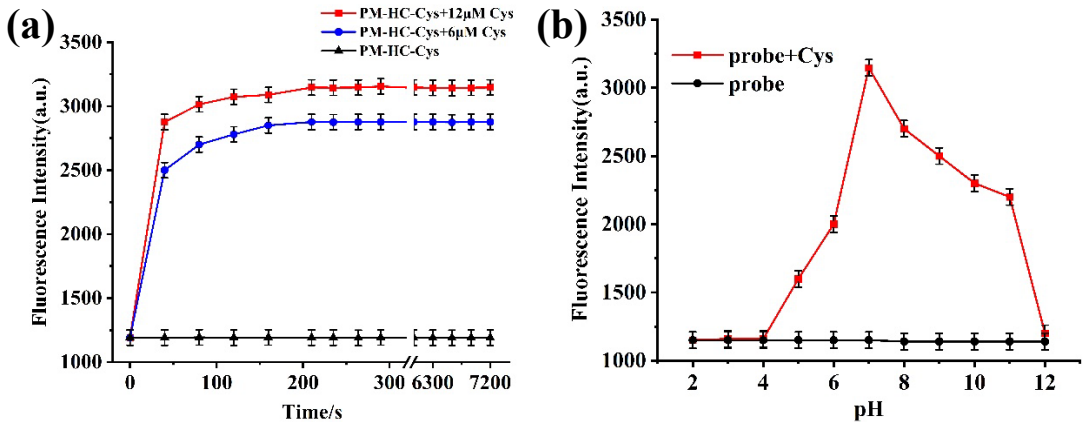

Figure S23. **(a)** Temporal variations in the fluorescence intensity of probe PH-Cys (10.0 μM) at 779 nm in DMSO/PBS (7:3, v/v), recorded in the absence and presence of cysteine (Cys: 6.0 μM and 12.0 μM). **(b)** Fluorescence intensity of probe PH-Cys (10.0 μM) at 779 nm across a pH range of 2.0-12.0 in DMSO/PBS (7:3, v/v), measured both prior to and following Cys supplementation.

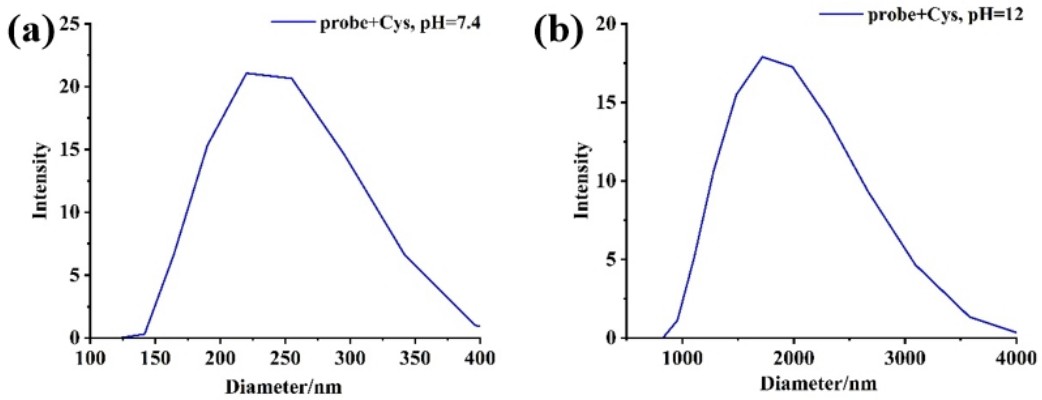

Figure S24. The particle size of probe PH-Cys (10.0 μM) following the addition of Cys in DMSO/PBS (7:3, v/v) was measured at **(a)** pH = 7.4 and **(b)** pH = 12.

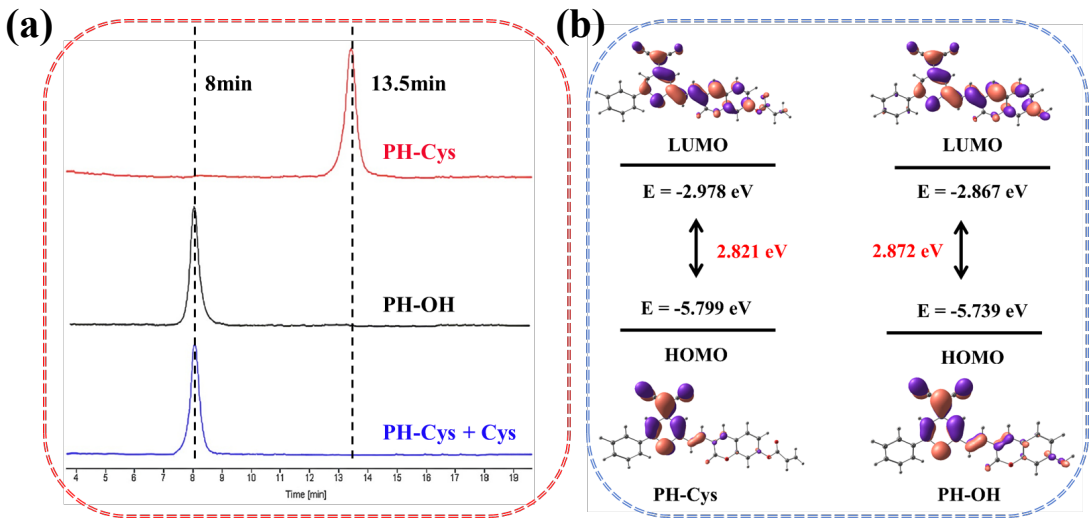

Figure S25. (a) Results of the PH-Cys and Cys reaction process monitored by HPLC.

(b) Frontier molecular orbitals of PH-Cys and PH-OH.

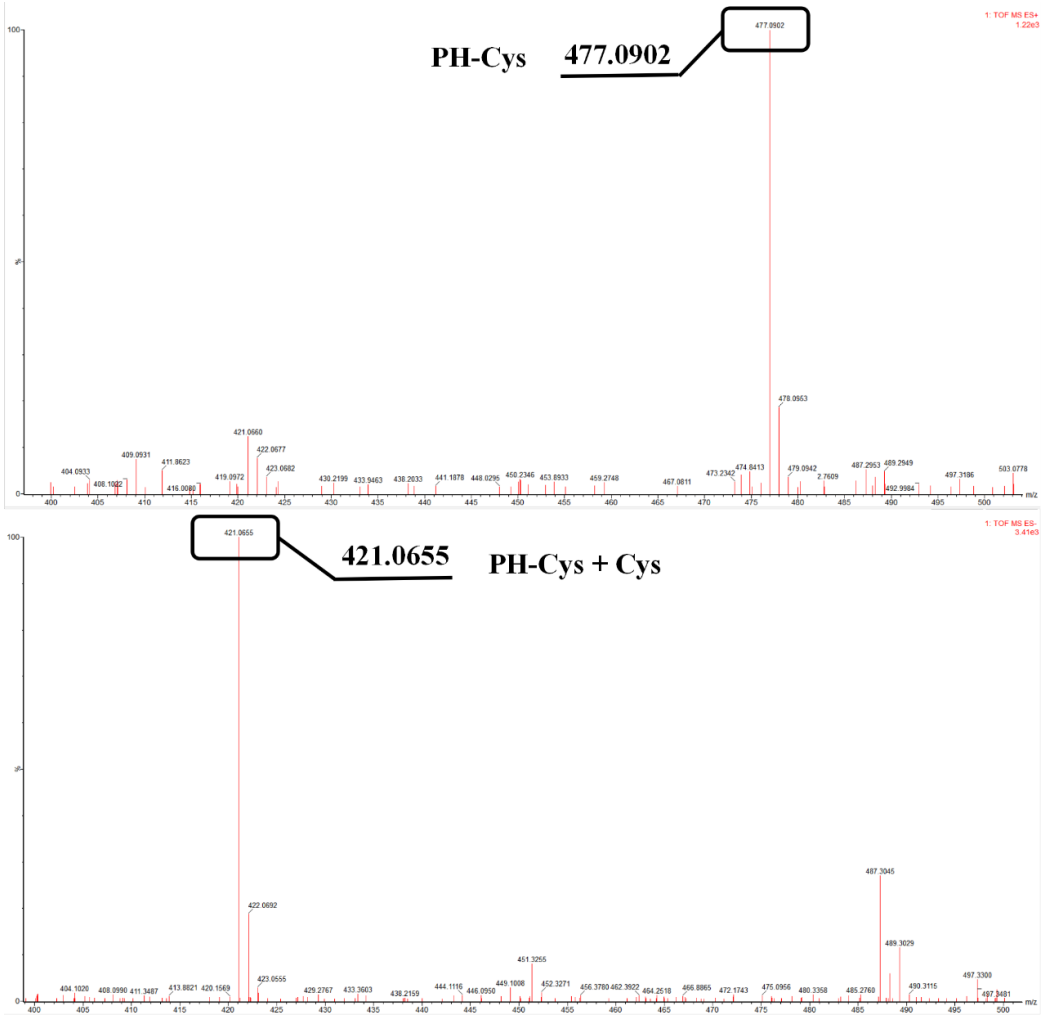

Figure. S26. Mass spectrum of PH-Cys and the addition of Cys.

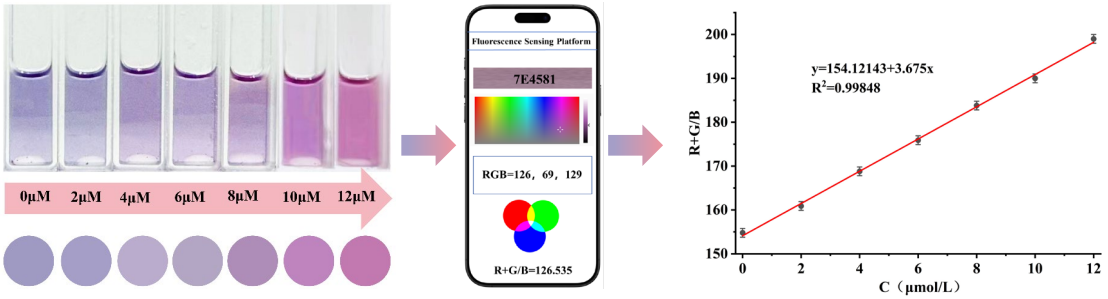

Figure S27. Diagram illustrating the determination of RGB values of solution color via smartphone-based measurement, depicting the color variation of PH-Cys probe with the change of Cys concentration in the range of 0 μM to 12.0 μM, as well as the linear correlation between the R+G/B ratio (R, G, B represent red, green, blue channels respectively) and Cys concentration within the range of 0 μM to 12.0 μM.

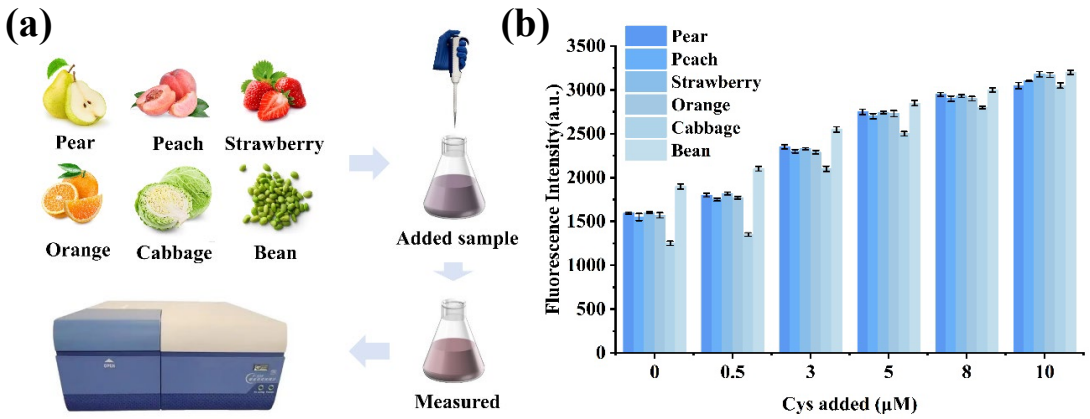

Figure S28. (a) Detection of Cys in real samples. **(b)** Changes in fluorescence intensity of probe PH-Cys upon the addition of Cys at different concentrations in actual samples.

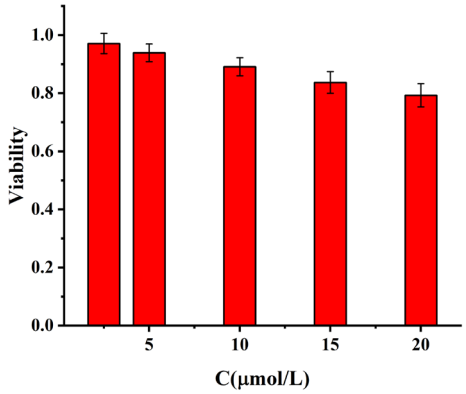

Figure S29. Cytotoxicity of probe PH-Cys.

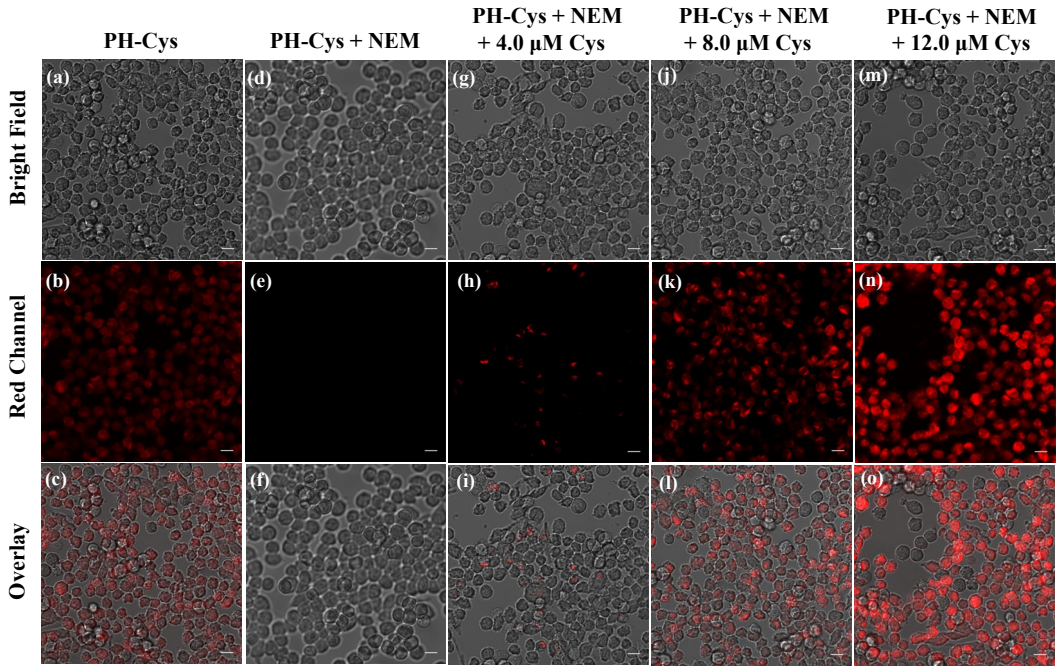

Figure S30. Confocal laser scanning microscopy (CLSM) images of cells stained with probe PH-Cys (10.0 μM). **(a)** Brightfield image of RAW 264.7 cells co-stained with PH-Cys alone; **(b)** Fluorescence image of the cells in **(a)** acquired under the red channel; **(c)** Merged image of **(a)** and **(b)**. **(d)** Brightfield image of RAW 264.7 cells co-stained with PH-Cys and pretreated with N-ethylmaleimide (NEM); **(e)** Fluorescence image of the cells in **(d)** acquired under the red channel; **(f)** Merged image of **(d)** and **(e)**. **(g)** Brightfield image of RAW 264.7 cells co-stained with PH-Cys, pretreated with NEM, and subsequently treated with 4.0 μM cysteine (Cys); **(h)** Fluorescence image of the cells in **(g)** acquired under the red channel; **(i)** Merged image of **(g)** and **(h)**. **(j)** Brightfield image of RAW 264.7 cells co-stained with PH-Cys, pretreated with NEM, and subsequently treated with 8.0 μM Cys; **(k)** Fluorescence image of the cells in **(j)** acquired under the red channel; **(l)** Merged image of **(j)** and **(k)**. **(m)** Brightfield image of RAW 264.7 cells co-stained with PH-Cys, pretreated with NEM, and subsequently

treated with 12.0 μM Cys; **(n)** Fluorescence image of the cells in **(m)** acquired under the red channel; **(o)** Merged image of **(m)** and **(n)**. (Excitation wavelength, λ_{ex} = 561 nm; Emission wavelength range, λ_{em} = 650-750 nm; Scale bar: 10 μm.)

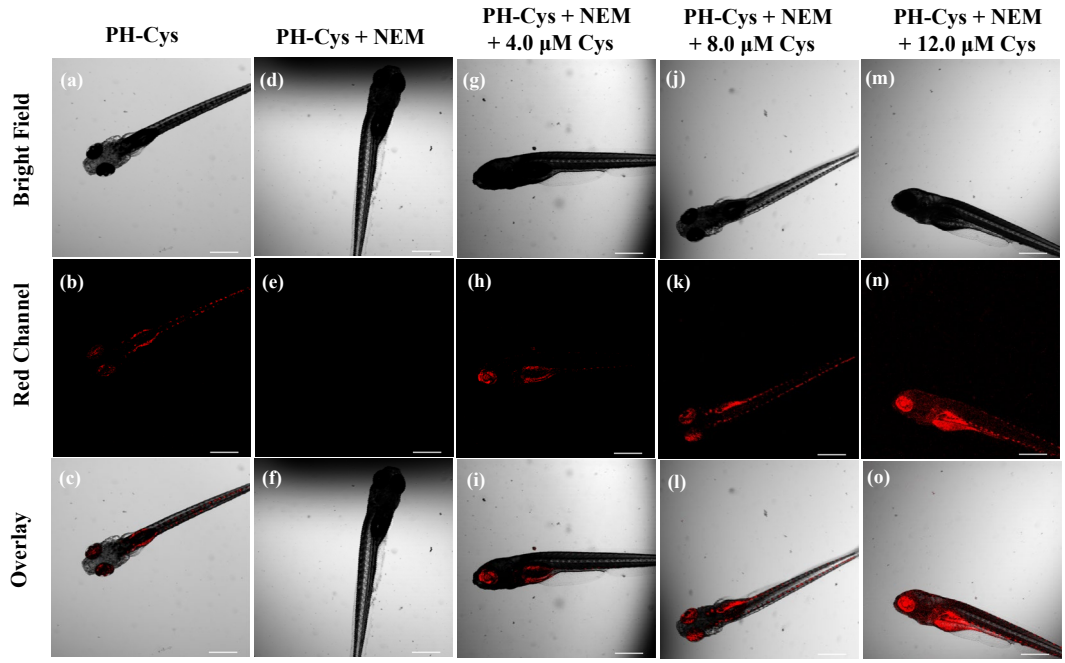

Figure S31. Confocal laser scanning microscopy (CLSM) images of zebrafish stained with probe PH-Cys (10.0 μM). **(a)** Brightfield image of zebrafish co-stained with PH-Cys alone; **(b)** Fluorescence image of the zebrafish in **(a)** acquired under the red channel; **(c)** Merged image of **(a)** and **(b)**. **(d)** Brightfield image of zebrafish co-stained with PH-Cys and pretreated with N-ethylmaleimide (NEM); **(e)** Fluorescence image of the zebrafish in **(d)** acquired under the red channel; **(f)** Merged image of **(d)** and **(e)**. **(g)** Brightfield image of zebrafish co-stained with PH-Cys, pretreated with NEM, and subsequently treated with 4.0 μM cysteine (Cys); **(h)** Fluorescence image of the zebrafish in **(g)** acquired under the red channel; **(i)** Merged image of **(g)** and **(h)**. **(j)** Brightfield image of zebrafish co-stained with PH-Cys, pretreated with NEM, and subsequently treated with 8.0 μM Cys; **(k)** Fluorescence image of the zebrafish in **(j)**

acquired under the red channel; **(l)** Merged image of **(j)** and **(k)**. **(m)** Brightfield image of zebrafish co-stained with PH-Cys, pretreated with NEM, and subsequently treated with 12.0 μM Cys; **(n)** Fluorescence image of the zebrafish in **(m)** acquired under the red channel; **(o)** Merged image of **(m)** and **(n)**. (Excitation wavelength, λ_{ex} = 561 nm; Emission wavelength range, λ_{em} = 650-750 nm; Scale bar: 500 μm.)

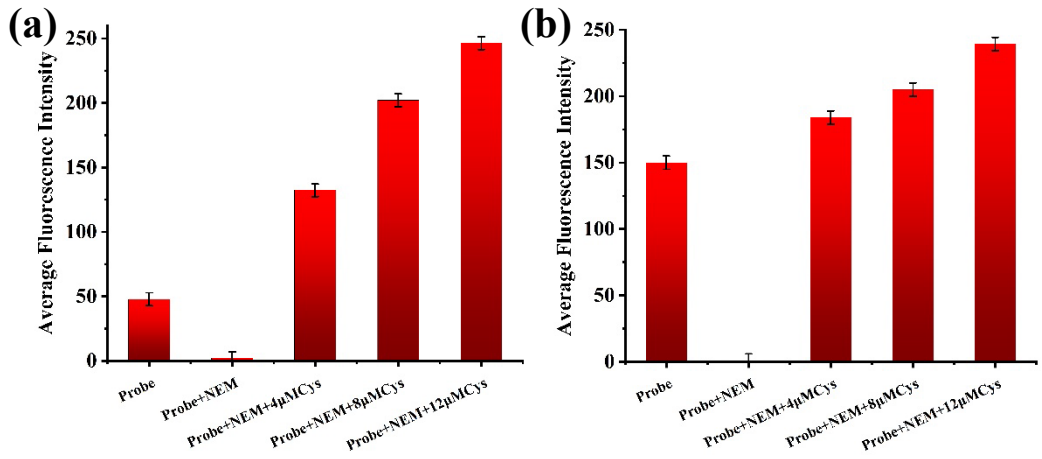

Figure S32. (a) Average fluorescence intensity in the red channel of confocal laser scanning microscopy (CLSM) images of RAW 264.7 cells. **(b)** Average fluorescence intensity in the red channel of confocal laser scanning microscopy (CLSM) images of zebrafish.

Table S1. Determination of Cys concentration in different samples.

Samples	Cys added (μM)	Found (μM)	Recovery (%)	RSD (n=5, %)	HPLC (μM)
Pear	0	1.26 ± 0.03	/	/	1.27 ± 0.02
	0.5	1.80 ± 0.07	108.11	4.30	1.78 ± 0.07
	3.0	4.30 ± 0.08	101.34	4.31	4.26 ± 0.09
	5.0	6.34 ± 0.10	101.63	4.11	6.33 ± 0.06
	8.0	9.22 ± 0.03	99.55	4.35	9.23 ± 0.03
	10.0	11.22 ± 0.15	99.61	4.32	11.19 ± 0.10

Peach	0	1.08 ± 0.16	/	/	1.00 ± 0.10
	0.5	1.61 ± 0.04	106.34	4.01	1.60 ± 0.04
	3.0	4.10 ± 0.07	100.69	3.90	4.11 ± 0.07
	5.0	6.02 ± 0.09	98.85	3.98	6.05 ± 0.07
	8.0	9.00 ± 0.07	99.07	4.08	8.90 ±0.10
	10.0	11.65 ± 0.02	105.72	4.12	11.65 ± 0.04
Strawberry	0	1.30 ± 0.03	/	/	1.28 ± 0.06
	0.5	1.83 ± 0.05	106.22	3.82	1.88 ± 0.03
	3.0	4.25 ± 0.12	98.39	3.98	4.25 ± 0.10
	5.0	6.24 ± 0.05	98.81	3.67	6.30 ± 0.05
	8.0	9.30 ± 0.10	100.12	3.69	9.33 ± 0.05
	10.0	11.34 ± 0.09	100.44	3.99	11.33 ± 0.09
Orange	0	1.13 ± 0.11	/	/	1.12 ± 0.09
	0.5	1.65 ± 0.05	104.13	2.20	1.60 ± 0.07
	3.0	4.10 ± 0.12	99.10	2.21	4.15 ± 0.03
	5.0	6.12 ± 0.14	99.89	2.07	6.15 ± 0.10
	8.0	9.11 ± 0.11	99.80	2.11	9.16 ± 0.06
	10.0	11.20 ± 0.07	100.76	2.25	11.19 ± 0.08
Cabbage	0	0.21 ± 0.03	/	/	0.20 ± 0.07
	0.5	0.70 ± 0.06	98.50	2.76	0.70 ± 0.01
	3.0	3.24 ± 0.06	101.06	2.28	3.19 ± 0.09
	5.0	5.10 ± 0.08	98.10	2.67	5.22 ± 0.08
	8.0	8.22 ± 0.09	100.15	2.78	8.11 ± 0.10
	10.0	10.19 ± 0.06	99.90	2.56	10.21 ± 0.07
Bean	0	2.56 ± 0.14	/	/	2.55 ± 0.10
	0.5	3.05 ± 0. 15	98.14	4.42	3.10 ± 0.14
	3.0	5.56 ± 0.16	100.11	4.12	5.57 ± 0.16
	5.0	7.60 ± 0.15	100.88	4.50	7.66 ± 0.19
	8.0	10.52 ± 0.16	99.56	4.39	10.40 ± 0.14
	10.0	12.49 ± 0.18	99.36	4.49	12.50 ± 0.19

Table S2. Comparison of properties of PH-Cys with reported Cys fluorescent probes.

Probe	λ_{ex}	λ_{em}	LOD	Time	Application	Rf
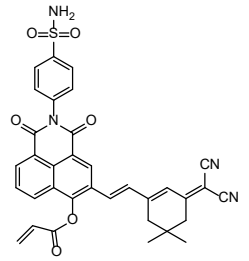	560 nm	684 nm	24 nM	35 min	cell imaging, zebrafish imaging and mice imaging	[1]
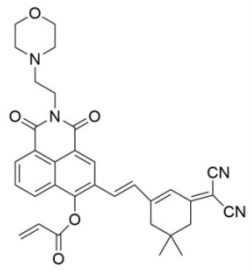	540 nm	688 nm	36 nM	3 min	cell imaging, zebrafish imaging and mice imaging	[2]
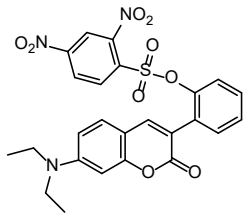	385 nm	478 nm	65 nM	8 min	cell imaging	[3]
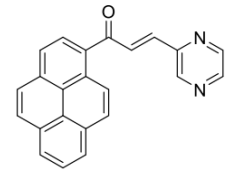	239 nm	391 nm	170 nM	5 min	cell imaging	[4]
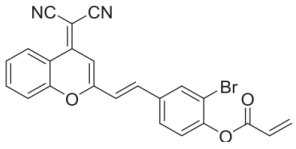	545 nm	760 nm	370 nM	30 min	cell imaging and mice imaging	[5]
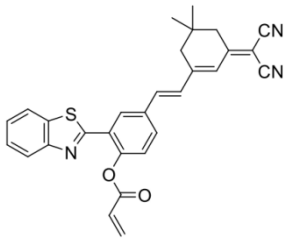	420 nm	660 nm	506 nM	60 min	cell imaging	[6]
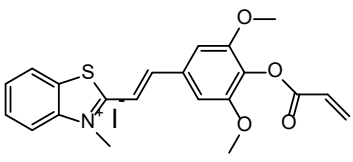	360 nm	560 nm	60.4 nM	20 min	cell imaging	[7]

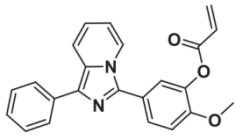	360 nm	502 nm	9 nM	15 min	cell imaging	[8]
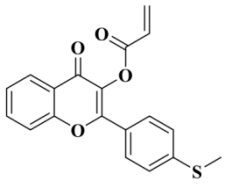	337 nm	450 nm	320 nM	90 s	Smartphone, test paper and cell imaging	[9]
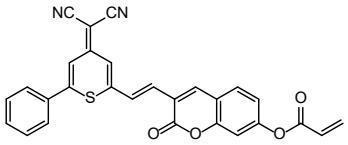	562 nm	779 nm	13.60 nM	3.0 min	Smartphone, cell imaging, zebrafish imaging and fruit samples	This work

References

1 Y. Lian, Y. Hou, Q. Ma, G. Mao, S. Hou, Y. Ma, N. Cui, R. Xia, *J. Photochem. Photobiol. A-Chem.*, 2025, **468**, 116512.

2 S. Hou, J. Xu, Q. Ma, G. Mao, Y. Ma, Y. Lian, C. Ning, R. Xia, *J. Pharm. Biomed. Anal.*, 2025, **265**, 116987.

3 B. Wang, S. Wang, H. Zhao, G. Yu, X. Liu, *Microchem J.*, 2025, 114793.

4 M. Wang, J. Du, Y. Ye, G. Lin, C. Liang, and W. Liu, *J. Mol. Struct.*, 2025, **1337**, 142095.

5 P. Cheng, H. Gong, H. Zhou, W. Luo, Y. Zhao, *Spectroc. Acta Pt. A-Molec. Biomolec. Spectr.*, 2026, **344**, 126677.

6 Y. Zhang, S. Zhao, H. Wang, C. Ge, *J. Mol. Struct.*, 2025, **1341**, 142684.

7 Z. Tang, M. Zhang, F. Yang, Y. Chen, T. Wang, Z. Chen, R. Yu, *Talanta*, 2025, **291**, 127870.

8 X. Jiang, B. Lin, H. Xia, J. Zhang, W. Huang, C. Wang, *J. Photochem. Photobiol. A-Chem.*, 2025, **462**, 116186.

9 X. Mei, X. Yuan, Y. Yang, L. Liu, Y. Lin, L. Xie, X. Chai, K. Xu, G. Du, L. Zhang, *J. Mol. Struct.*, 2024, **1312**, 138486.